INFRARED EXCITATION OF MOLECULES AND CLUSTERS

MARCEL SNELS

INFRARED EXCITATION OF MOLECULES AND CLUSTERS

INFRARED EXCITATION OF MOLECULES AND CLUSTERS

PROEFSCHRIFT

TER VERKRIJGING VAN DE GRAAD VAN DOCTOR
IN DE WISKUNDE EN NATUURWETENSCHAPPEN
AAN DE KATHOLIEKE UNIVERSITEIT TE NIJMEGEN
OP GEZAG VAN DE RECTOR MAGNIFICUS
PROF. DR. J. H. G. I. GIESBERS
VOLGENS BESLUIT VAN HET COLLEGE VAN DEKANEN
IN HET OPENBAAR TE VERDEDIGEN
OP WOENSDAG 18 JUNI 1986
DES NAMIDDAGS TE 4 UUR PRECIES

door

MARCELLINUS NICOLAAS NORBERTUS SNELS

geboren te Tilburg

krips repro meppel

1986

Promotor: Prof. dr. J. Reuss

Op deze plaats wil ik iedereen die direct of indirect heeft meegewerkt aan het tot stand komen van dit proefschrift bedanken, en met name

de (oud-) medewerkers van de afdeling Atoom- en Molecuulfysica, voor de prettige samenwerking.

Coen Liedenbaum en Rick Sanders, die in hun afstudeertijd een bijdrage hebben geleverd aan dit onderzoek.

Cor Sikkens, Frans van Rijn, John Holtkamp en Eugene van Leeuwen voor hun zeer gewaardeerde technische assistentie.

Leo Hendriks voor het vervaardigen van alle tekeningen in dit proefschrift.

Annette van der Heijden voor haar hulp bij het voltooien van het manuscript.

De hoofden van de dienstverlenende afdelingen van de Faculteit der Wiskunde en Natuurwetenschappen, met name P. Walraven, H. Verschoor, W. Schut, J. Holten, R. Gelsing, H. Spruyt en J. van Langen.

per Roberta
per la piccola peste

CONTENTS

This thesis is a collection of five articles about the interaction of IR laser radiation (9 - 11μm) with molecules and clusters

The first chapter is the result of two visits of four months altogether, to the Laboratory of Molecular Spectroscopy, at Frascati, Italy Multiple photon excitation of SiH_4 in a low pressure opto-acoustic cell was examined A continuously tunable CO_2 TE laser was used to excite the SiH_4 molecules in a one- or multiple-photon process After comparison with the well known linear absorption spectrum, multiple photon transitions could be identified Calculations by C I and G Pierre made it possible to assign several two-photon transitions [1]

The other four chapters in this thesis deal with the excitation of small clusters In a molecular beam small complexes of C_2H_4, NH_3, SF_6, SiF_4 and SiH_4 were produced Beam conditions were optimized to favour the production of dimers A line tunable CO_2 laser was used to excite the formed clusters Absorption of one photon is followed by a rapid dissociation, the dissociation fragments disappear from the beam axis, which results in a decrease of the beam signal Small (laser induced) variations of the molecular beam intensity (about one part in $5 \cdot 10^6$) could be observed due to a sensitive bolometer, which was placed rather close (400 mm) to the interaction point of laser and molecules Using phase sensitive techniques dissociation spectra were obtained, which show rather broad (FWHM = 2 - 12 cm^{-1}) structures The observed linewidth has been related to transitions involving the excitation of internal degrees of freedom of the complex The linewidth of these transitions yields a lower limit of the pre-dissociation lifetime of the excited cluster

In the dimer spectrum of C_2H_4 combination bands of the ν_7-vibration with a van der Waals mode have been observed Hot-band transitions due to the same van der Waals mode were predicted, and have been observed recently in Gottingen by Buck et al [2] Observation of rotational fine structure with a linewidth of 10 MHz (FWHM) sets a lower limit of 16 ns for the lifetime of the excited dimer Present experimental data are supported by recent calculations of Hutson et al [3] which predict a lifetime of $\simeq 5 \cdot 10^{-6}$s for the C_2H_4 dimers

The IR-dissociation of NH_3 dimers provided evidence that the two NH_3 molecules in the complex are not equivalent Furthermore, a tunneling motion is

held responsible for a splitting in ground- and excited states of the dimer. This assumption leads to a satisfying explanation of the observed spectra.

The structure of dimers constitued by high symmetry molecules, (like SF_6, SiF_4 and SiH_4) is mainly determined by the intermolecular distance R. Taking into account the resonant dipole-dipole interaction for the excited complexes allowed a satisfactory fit of the observed spectra, except for SiH_4. The linewidth of the spectral structures of SF_6- and SiF_4 dimers could be reproduced rather well, if one allows free rotation of the molecules in the complex.

Some mixed clusters have also been investigated and spectral information on the NH_3-SiH_4 dimer has been obtained for the first time.

Finally, saturation effects for the dissociation of SF_6 dimers are discussed in a theoretical paper.

Small clusters of light molecules, like C_2H_4 and NH_3 dimers, may be present in the atmosphere of the cold planets of the solar system and in the interstellar space, they may also escape from the nucleus of comets. Apart from their astrophysical interest, the present experiments may be relevant for laser induced isotope separation processes (see chapter 1 and 4).

References

[1] C.I. Pierre and G. Pierre, private communication

[2] F. Huisken and U. Buck, private communication

[3] A.C. Peet, D.C. Clary and J.M. Hutson, private communication

MULTIPLE-PHOTON EXCITATION SPECTRA OF SiH_4 MEASURED IN THE 10 μm RANGE BY A CONTINUOUSLY TUNABLE CO_2 LASER

M SNELS [1], R LARCIPRETE [2], R FANTONI, E BORSELLA and A GIARDINI-GUIDONI
ENEA Dipartimento TIB CRE C P 65 00044 Frascati Rome Italy

Received 24 August 1985 in final form 8 October 1985

SiH_4 absorption of 10 μm laser radiation from a continuously tunable CO_2 laser has been measured The occurrence of multiple photon excitation has been shown from comparison with linear absorption spectra and from the dependence of some peak intensities upon laser fluence

1. Introduction

In the present paper SiH_4 laser excitation has been investigated in the 10 μm region by using a continuously tunable pulsed CO_2 laser Nowadays interest in studying the mechanism of SiH_4 laser excitation arises because this molecule is the starting material for most thin-film silicon deposition and silicon-containing powder production [1] While in the past thin films were produced via plasma-enhanced chemical vapour deposition (CVD) and special silicon powder by conventional gas-phase chemical reaction after SiH_4 pyrolysis [2], more recently several methods utilizing IR laser photolysis of SiH_4 are developing for both processes of industrial interest In fact effective heating of SiH_4 molecules up to their decomposition threshold can be achieved when a gaseous sample is irradiated by laser radiation tuned over the CO_2 10 μm branches

Due to the peculiarity of both SiH_4 infrared absorption spectra (see next paragraph) and to the unusual experimental conditions under which SiH_4 is irradiated to produce the required thin films or powders [3,4], it is of great interest to investigate the mechanism through which the laser excitation occurs

Up to now the occurrence of IR multiple-photon excitation up to dissociation threshold has been demonstrated on many different polyatomic molecules [5] In particular at room temperature the importance of a crowded rotational manifold in overcoming the anharmonic bottleneck has been shown [6,7], while at low temperature (in supersonic beam experiments) the role of pure vibrational levels and sublevels in each excitation ladder has been recognized [8]

In the IR photolysis of SiH_4 at room temperature it is important to understand the effect of collisions on the photodissociation process It has been observed [9] that collisions are effective in increasing both the absorption probability and the dissociation yield Provided that the collisions are not effective in increasing the absorption of the first few photons, a true coherent excitation occurs [5], otherwise the process involves a full thermodynamic redistribution of absorbed energy through fast intermolecular relaxations The observation in ref [10] of a sharply structured SiH_4 absorption spectrum after irradiation by a line-tunable CO_2 laser suggested an IR multiple-photon excitation The present investigation, carried out with a continuously tunable CO_2 laser in different pressure and fluence ranges, will throw more light on possible two- and three-photon resonant absorption in SiH_4

[1] Also at Fysisch Laboratorium Katholieke Universiteit Toernooiveld 6525 ED Nijmegen The Netherlands
[2] ENEA guest

2 SiH_4 IR absorption spectrum

In comparison with much studied molecules as SF_6, CF_3Br, CF_3I and others, SiH_4 has a very large rotational constant (B_e = 2 86 cm^{-1}) [11], which exceeds the laser resolution (0 12–0 15 cm^{-1}) and the expected power broadening (<0 1 cm^{-1} for 10^6 W/cm^2) This means that the rotational manifolds of the strong IR-active ν_4 vibrational mode and the IR-inactive ν_2 vibration give a very broad absoption spectrum from 850 to 1100 cm^{-1} at room temperature [12,13] The IR-forbidden ν_2 vibration (972 1 cm^{-1}) becomes partially IR-allowed through a strong Coriolis interaction with the ν_4 mode (913 3 cm^{-1}), and appears clearly in the linear absorption spectrum First-order Coriolis interaction, splitting the levels of the three fold degenerate ν_4 mode, has to be included in a simple ν_2, ν_4 energy-level scheme which can be used to calculate multiple-photon resonances excited by 10 μm laser radiation

$$E_{v,J}^{(2,4)} = v_2\omega_2 + v_2(v_2 - 1)\chi_{22} + v_4\omega_4$$

$$+ v_4(v_4 - 1)\chi_{44} + v_2v_4\chi_{24} + BJ(J-1) + F_{\zeta_4}\,, \quad (1)$$

where F_{ζ_4} is the ν_4 Coriolis splitting and has the values [14]

$$F_{\zeta_4}^{(-)} = 2B\zeta_4(J+1)\,, \quad F_{\zeta_4}^{(0)} = -2B\zeta_4\,,$$

$$F_{\zeta_4}^{(+)} = -2B\zeta_4 J$$

Even by using this strongly approximated expression, neglecting higher-order terms such as anharmonic splitting in the tetrahedral field and centrifugal distortions [15], and taking into account only an effective B value avaraged over the molecular vibrations, it is not possible to predict multiple-photon resonances In fact, among the constants appearing in the abovementioned energy level expression, besides ν_2 and ν_4, only the value of the rotational constant B and of the Coriolis interaction in the ν_4 mode are known (ζ_4 = 0 50) [12] In particular the anharmonicity constant χ_{44} is unknown, due to the fact that for symmetry reasons (ν_4 is a perpendicular vibration of a spherical top molecule) the intensity of the $0 \rightarrow 2$ transition in the ν_4 mode is expected to be very weak (only the F_2 component is allowed) Apart from IR Fourier transform measurements [16], this missing value could be obtained either measuring the $0 \rightarrow 3$ overtone transition as has been done for the ν_3 mode of SF_6 in a multipass cell with a diode laser [17], or measuring in a double-resonance experiment the ν_4 $1 \rightarrow 2$ hot band (an analogous measurement has been done on SF_6 [18] and CH_4 [19]) Another alternative is to measure directly the ν_4 $0 \rightarrow 2$ overtone in a Raman spectroscopy experiment [20].

Since the excited level scheme of SiH_4 is not known, present data, measured with the apparatus described in section 3 and reported in section 4, are discussed only on the basis of available high-resolution linear absorption data [12] Even without a theoretical treatment, some useful results have been obtained which can help us to understand the process of laser-induced SiH_4 photodissociation, as explained in the conclusion of this paper (section 5)

3 Experimental

For an investigation of significant portions of the absorption spectra in which multiple-photon excitation could be observed, it is necessary to use a high-power continuously tunable laser together with a senstive detection system In our apparatus, sketched in fig 1, the continuously tunable radiation was provided by a commercial (Lumonics model TE 281) multimode pulsed source operating at 10 atm Due to high reflectivity optics, the laser was operated just above threshold, originating a quasi-single-mode initial pulse, followed by a short multimode tail (400 ns) [6] The initial pulse (100 ns fwhm) contained half of the total energy The laser resolution was measured to

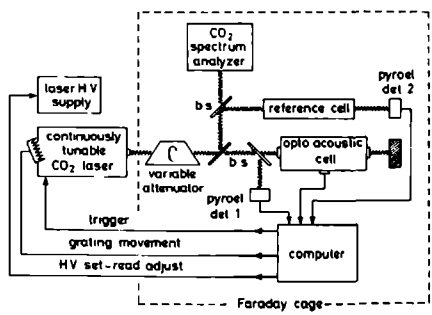

Fig. 1. The apparatus

be 0 12 ± 0 02 cm^{-1} The laser ouput energy was monitored after a 10% beam-splitter by a pyroelectric detector (Lumonics model 20D) The intensity of the laser pulse could be monitored by means of a fast detector (Molectron P3) The frequency calibration was accomplished by measuring the attenuation spectrum on another fraction of the laser beam sent to a reference cell (1 m long) filled with several tenths of a Torr of NH_3 and then to a second pyroelectric detector The NH_3 linear spectrum is characterized by several well resolvable peaks in the 10 μm region [21], corresponding to symmetric and asymmetric ν_2 vibrorotational transitions

In order to reveal the presence of possible small features in the non-linear excitation spectra of SiH_4, a previously described [22] opto-acoustic cell has been used to measure the absorption This device works on the principle that the maximum of the opto-acoustic signal envelope is proportional to the average energy absorbed by the molecules The calibration of the microphone response was accomplished, at fixed fluences, by measuring the beam attenuation in the same cell by means of two calibrated pyroelectric detectors Furthermore, since the opto-acoustic signal may not be completely linear with the absorbed energy if the laser fluence is varied over one order of magnitude [22], the measurements of absorbed energy versus laser fluence have also been done with the conventional attenuation technique Variations in laser fluence have been obtained using beam splitters and rotating Brewster plates, so that the time profile of the laser pulse was unchanged All the measurements were performed at room temperature, although the opto-acoustic cell can be cooled [7], because SiH_4 cold spectra would be shifted out of the CO_2 laser emission

Great care has been taken to shield very carefully the apparatus from the laser discharge noise The experiment was computer controlled by a TMS 9900 based microcomputer taking care of data acquisition and processing The computer also set the laser output energy within a small range by varying the laser discharge energy (HV power supply) and moving the laser emission frequency through a synchronous motor mounted on the grating

A deposition cell, in which slices of different materials could be placed close (parallel or perpendicular geometry) to the laser radiation and heated to 400°C by a suitable resistor, has also been used to obtain film and powder depositions Experiments have been performed at different SiH_4 pressures in the presence of additional Ar or N_2 as buffer gas The gaseous sample has been irradiated by using both the pulsed source (Lumonics TEA model 102) and a CO_2 cw laser (Molectron model IR 250) Fluorescence emitted in the SiH_4 decomposition process has been observed in the deposition cell A detailed study of this fluorescence will be the subject of a forthcoming paper [23]

4 Results and discussion

Preliminary measurements of SiH_4 spectra were performed in this apparatus by substituting the continuously tunable source with the line-tunable TEA CO_2 laser Spectra similar to the one reported in ref [10] have been measured at a laser fluence $\phi = 0\ 3$ J/cm^2 at different SiH_4 pressures The average number of absorbed photons ($\langle n \rangle = 0\ 6$) measured on 1 Torr of gas at $\phi = 0\ 5$ J/cm^2 and $\omega = 944\ 2$ cm^{-1} (10P20) was in good agreement with ref [10]

In comparison with ref [10], a broader range of wavenumbers on the CO_2 R branch was scanned and an extra maximum between R32 and R34 was found The overall absorption measured on 1 Torr of SiH_4 in this region was lower than in the previous data [10], whereas the maximum on the 10R24 was much less pronounced Strong features, especially on the P branch, were found in all the investigated ranges These structures were still present when the overall pressure was increased to 11 Torr by adding Ar as a buffer gas Since a lot of linear transitions occur in SiH_4 between the CO_2 laser lines [12], it was impossible to discuss these roughly scanned spectra in terms of linear or non linear resonances

Absorption spectra of SiH_4 were obtained operating the continuously tunable CO_2 laser on the most intense parts of the 10 μm P and R branches and scanning the laser frequency in steps of about 0 05 cm^{-1} Two spectra measured on the P branch are shown in fig 2, while results obtained on the R branch are reported in fig 3 Data of figs 2 and 3 have been measured using the optoacoustic cell filled with 1 Torr of pure SiH_4 at two different laser fluences, 0 13 J/cm^2 (a) and 0 05 J/cm^2 (b) Error

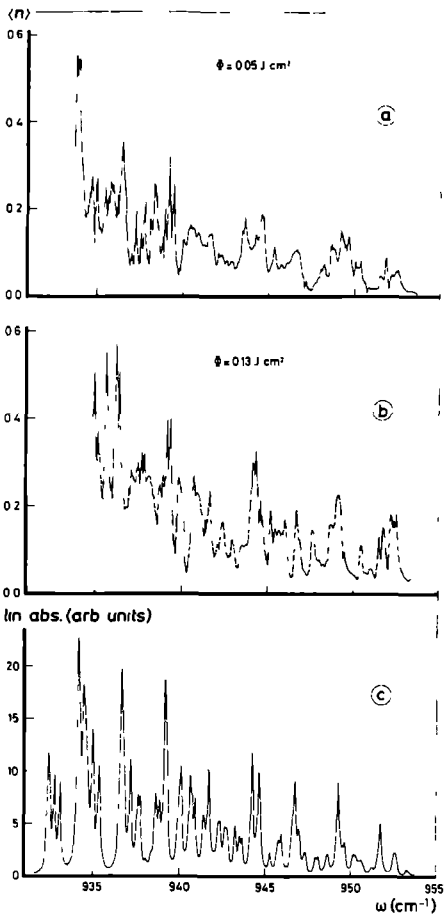

Fig. 2. SiH_4 (p = 1 Torr) opto-acoustic spectra measured on the 10 μm CO_2 P branch at ϕ = 0.13 J/cm^2 (a) and at ϕ = 0.05 J/cm^2 (b), compared with the reconstructed linear absorption spectrum (c).

bars on each data point were between ±5% and ±10% of the measured value. At the bottom of the same figures (c) a linear absorption spectrum of SiH_4, calculated for the present experimental conditions, is shown for comparison. This spectrum is based on linear absorption data [12], using for each transition

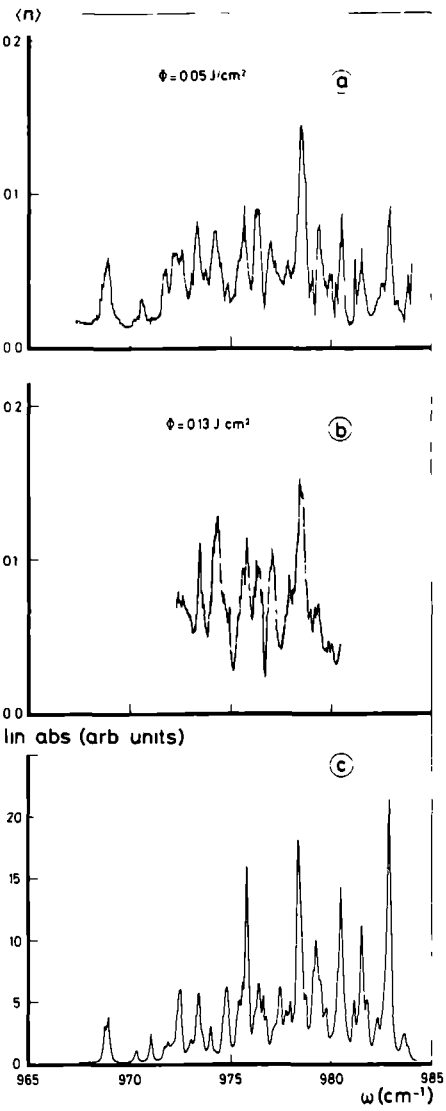

Fig. 3. SiH_4 (p = 1 Torr) opto-acoustic spectra measured on the 10 μm CO_2 R branch at ϕ = 0.13 J/cm^2 (a) and at ϕ = 0.05 J/cm^2 (b), compared with the reconstructed linear absorption spectrum (c).

the measured position and calculated relative intensity (since some of them are not resolved in the Fourier transform IR spectra) [12,13] A Lorentzian profile for the absorption lines has been assumed, the laser resolution as well as the power broadening occurring at $\phi = 0.05$ J/cm^2 have been taken into account Those factors are mainly responsible for the width measured on each peak (pressure broadening at $p =$ 1 Torr is negligible)

Both spectra have some general features in common The average number of absorbed photons per molecule, calibrated as discussed in section 3, is rather low, being almost an order of magnitude lower than in heavier molecules, e g CF_3I [7] and SF_6 [24] An explanation could be that when the first few vibrational levels of SiH_4 are excited with low laser intensity ($I < 1$ MW/cm^2), each sublevel of the rotational manifold contributes to a single transition, in most cases well resolved from all others of the same species If this excitation scheme holds, the rotational relaxation during the laser pulse cannot be effective in increasing the absorption in the first vibrational levels at any fixed frequency ($\Delta\nu = 0.12$ cm^{-1} against $2B =$ 5.72 cm^{-1}) For the same reason saturation of the single vibrorotational linear transition should quite easily be observed

By comparing data in figs 2 and 3 with the calculated linear spectrum, there are some extra peaks Their intensities are strongly sensitive to the laser fluence (i e to the laser intensity, since the time profile of the laser pulse does not change), and they are superimposed on a saturated linear absorption spectrum Most of the extra peaks appear in fig 2, where the frequency region from 933 to 954 cm^{-1} is scanned The spectra reported in fig 3 (968–984 cm^{-1}) seem to reproduce mainly saturated linear absorption Table 1 gives the frequency position together with the measured width (fwhm) for the extra peaks

We give a short comment about differences between the results shown in figs 2 and 3, i e why at the same fluence the extra peaks are more abundant on the low-frequency region of the spectrum In the low-frequency region (fig 2) linear transitions between vibrorotational levels of the ν_4 R branch ($8 \leqslant J \leqslant 18$) occur (see ref [12] for their assignment), whereas in the high frequency region (fig 3) transitions in the Q branch ($3 \leqslant J \leqslant 14$) of the IR forbidden ν_2 mode are dominant ($11 \leqslant J \leqslant 13$ R components of the ν_4 are also present) [12] The Coriolis coupling with ν_4 makes this mode weakly IR active, but its band intensity is much lower than ν_4 This fact should also affect the multiple-photon excitation probability, yielding only a few possible non-linear features in fig 3 This behaviour is in agreement with what has been observed in SF_6 [25] and C_2H_4 [26] weak IR bands (such as for instance overtones or combination bands) show a much higher threshold for the onset of multiple-photon excitation, as well as a lower cross section in single-frequency excitation

Data in fig 3 allowed us to ascertain that the sharp peak found by ref [10] at 978.5 cm^{-1} (10R24) cannot be a multiple-photon resonance Since saturation of this peak is clearly observed when laser fluence is increased, it appears to be a convolution of a few linear transitions (some Q(10) and Q(6) multiplets

Table 1
List of SiH_4 multiple-photon resonances observed in figs 2 and 3

Frequency (cm^{-1})	Measured width (cm^{-1})	Frequency (cm^{-1})	Measured width (cm^{-1})
933.84	0.38	944.32	0.17
934.73	0.22	947.68	0.23
935.12	0.22	947.78	0.30
935.76	0.22	950.49	0.33
936.19	0.28	951.54	0.21
936.40	0.16	952.22	0.23
938.12	0.16	952.57	0.12
938.26	0.18	970.58	0.42
938.97	0.13	974.25	0.68
939.42	0.14	977.00	0.44

falling between 978 3 and 978 5 cm^{-1} [12]) within the laser bandwidth (almost the same as for ref [10])

The occurrence of non-linear processes, producing the extra peaks shown in fig 2, has been checked measuring the behaviour of several structures varying the laser fluence over one order of magnitude without affecting the pulse time profile Although it is well known that the dependence on laser fluence is not the best way to investigate non-linearity [27], it has to be stressed that in the present experiment it was not possible to modify the pulse shape into a square single-mode pulse with variable length, as done for instance in ref [28] without losing the tunability Some typical results of the measurements performed by varying laser fluence are shown in figs 4a–4c where at the bottom (d) the corresponding enlarged section of the multiple-photon and linear spectra are reported In fig 4a the slope versus laser fluence has been measured on a linear peak which is the convolution of $R^-(13)$ and $R^-(15)$ multiplets [12]) at ω = 946 7 cm^{-1} In fact the expected slope ≈ 1 has been found in the fluence range from $1\,8 \times 10^{-2}$ to $5\,0 \times 10^{-2}$ J/cm^2, followed by linear absorption saturation (slope $\approx 0\,5$ [7]), and again the slope equals 1 in the higher fluence range from 7×10^{-2} to 3×10^{-1} J/cm^2 In fig 4b some non-linear contribution seems to be superimposed to the linear absorption peak at ω = 944 3 cm^{-1} ($R^-(12)$ multiplet [12]) A slope between 1 and 2 has been found in the fluence range from 8×10^{-2} to 4×10^{-1} J/cm^2, suggesting the presence of one or more two photon resonances A more complicated situation is shown in fig 4c, where the structure at ω = 947 7 cm^{-1}, which is absent in the linear spectrum, should be a convolution of two- and three-photon transitions falling within the laser resolution In fact there is initially a slope ≈ 2, then saturation for two-photon transition (slope ≈ 1 [7]), and finally the slope is $2.5 \pm 0\,5$ measured in the highest fluence range. In this case the onset of processes of different order and their respective saturation originate the step-like behaviour with several different slopes observed in different fluence ranges

In our opinion fig. 4 shows that the extra peaks observed on SiH_4 laser absorption spectra are IR multiple-photon resonances, for which the initial and final states on the ν_4 vibrorotational ladder are not known Preliminary results of investigations on $2\nu_2$, $\nu_2 + \nu_4$ and $2\nu_4$ [16] cannot be used to identify any of the final states for the transition listed in table 1, since the analysis is restricted to the 1961–1967 cm^{-1} range

In discussing the structures observed in the present spectra of SiH_4 it should be kept in mind that also population resonances on certain excited levels might be generated for high-intensity excitation (100–500 GW/cm^2) as the calculations performed in refs [29,30] for the O_3 molecule show These other resonances cannot be predicted on the simple basis of the positions of excited levels, since they occur as a consequence of quantum interference in the dynamical calculation Since present knowledge of SiH_4 excited states is not even sufficient to predict the resonances in a multistep scheme, calculations like the ones suggested by Quack and Sutcliffe [29,30] to investigate the occurrence of population resonances in SiH_4 are not yet possible Comparison of the intensity at which the present experimental data have been measured with those of the spectra calculated in ref [30], shows that we are far from measuring such effects This hypothesis is also supported by the presence in figs 2 and 3 of most of the linear absorption peaks, which in Quack's model could be cancelled by the occurrence of quantum interference phenomena

For practical applications it has to be emphasized that one of the non-linear structures found at ω = 944 3 cm^{-1} is on resonance with the 10P20 laser line which is commonly used as excitation frequency in laser induced photodecomposition

5 Conclusions

The present work has given the first experimental evidence of multiple photon excitation of SiH_4 molecules The non-linear excitation has been verified at low laser fluences 10^{-2}–10^{-1} J/cm^2 for a pressure range of 10^{-1}–1 Torr Under these conditions less than one photon per molecule is absorbed, at several laser frequencies this occurs through resonances absent in the linear spectrum Multiple-photon excitation seems to be important in the first step of the absorption also when a line tunable laser is used for excitation, since some non linear transitions are found in coincidence with the CO_2 emission lines of a low pressure laser source This is true especially in the case of the strong 10P20 laser line As already

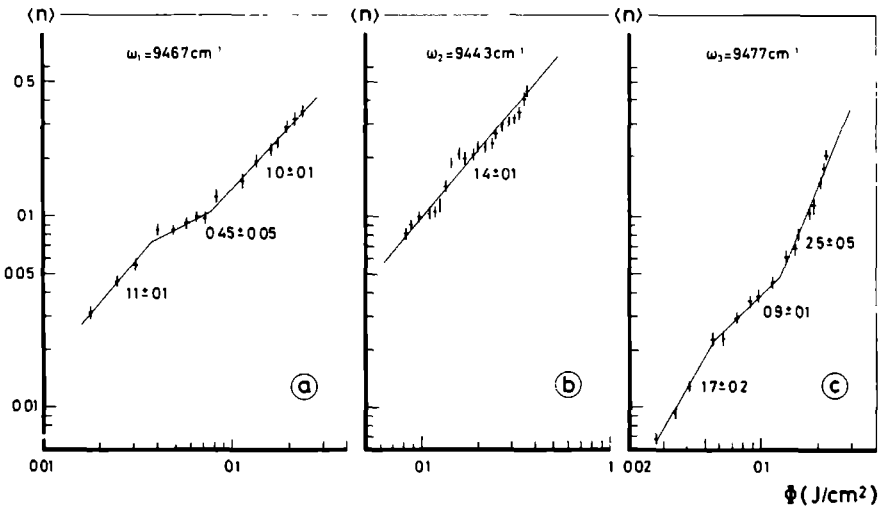

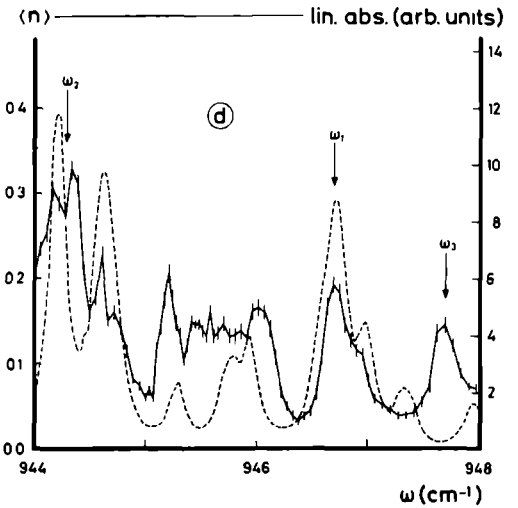

Fig. 4. SiH_4 (p = 1 Torr) absorption versus laser fluence measured at ω = 946.7 cm^{-1} (a), ω = 944.3 cm^{-1} (b) and ω = 947.7 cm^{-1} (c). In (d) enlarged sections of the multiple-photon spectrum measured at ϕ = 0.13 J/cm^2 (full line, left scale) and linear spectrum (dotted line, right scale) are also shown for comparison, arrows indicate different ωs.

suggested for a lot of heavier molecules, it is possible that after excitation through the first few levels the absorption process goes through a very crowded manifold of levels in which the collision-assisted redistribution of the absorbed energy may help to reach and overcome the dissociation threshold. A discussion of this point requires further investigation on the absorption of SiH_4 up to highly excited states

Furthermore, in the course of this work, dissociating SiH_4 by means of resonant laser absorption, experimental indications have been obtained that SiH_4 pressure and laser fluence affect strongly the physical and chemical properties of the deposit. In fact, in agreement with ref [31], our preliminary measurements performed in the cell mentioned in section 3, allowed us to observe that low pressure and low fluence favour the deposition of amorphous hydrogenated silicon films, while high pressure and high fluence produced mainly crystalline silicon powders. These results have been obtained both with a pulsed TEA CO_2 laser and with a continuous cw CO_2 laser tuned on 10P20

Further work is in progress monitoring the dissociation together with the absorption under different conditions of excitation in order to understand whether different processes occurring in the absorption of the first few photons can affect the properties of the final products in the deposition.

Acknowledgement

The authors gratefully acknowledge the help of R. Belardinelli throughout the experiments Technical assistance of P. Cardoni and G. Schina is also appreciated We thank Professor J Reuss for his useful comments on the manuscript One of us (MS) thanks the Italian CNR for the financial support on request of ZWO (Netherlands Organisation for the Advancement of Pure Research).

References

[1] J.T Yardley and A. Gupta, Laser-Produced Ultrafine Powders and Applications, paper presented on February 16, 1984 at the Electro-Optics/Laser International Exposition in Tokyo.

[2] M H Brodsky, ed., Plasma discharge amorphous semiconductors (Springer, Berlin, 1979).

[3] R. Bilenchi, I Gianinoni and M Musci, J. Appl Phys 53 (1982) 6479

[4] T J. Chuang, J Chem. Phys 74 (1981) 1453.

[5] C D. Cantrell, V S. Letokov and A.A. Makarov, in Coherent nonlinear optics, eds. M.S Feld and V.S Letokov (Springer, Berlin, 1980) p. 165;
A. Giardini-Guidoni, E. Borsella and R. Fantoni, Ber Bunsenges Physik Chem. 89 (1985) 286.

[6] E. Borsella, R. Fantoni, A. Giardini-Guidoni, D R Adams and C D. Cantrell, Chem. Phys Letters 101 (1983) 86

[7] U del Bello, E. Borsella, R. Fantoni, A Giardini-Guidoni and C D. Cantrell, Chem Phys Letters 114 (1985) 467.

[8] E Borsella, R Fantoni, A Giardini-Guidoni, D. Masci, A Palucci and J. Reuss, Chem Phys Letters 93 (1982) 523;
E. Borsella, R. Fantoni, L.Y. Shen and M. Nardelli, Nuovo Cimento 4D (1985) 548

[9] P A Longeway and F W. Lampe, J Am Chem. Soc. 103 (1981) 6813

[10] T F Deutsch, J. Chem. Phys. 70 (1979) 1187

[11] M Dang-Nhu, G. Pierre and R. Saint-Loup, Mol Phys 28 (1974) 447.

[12] D L Gray, A.G Robiette and J.W C Johns, Mol. Phys. 34 (1977) 1437

[13] G Pierre, A. Valentin and L Henry, Can J. Phys (1985), to be published

[14] J W C Johns, W A Kreiner and J Susskind, J Mol Spectry 60 (1976) 400.

[15] A.G Robiette, D.L Gray and F W. Birss, Mol. Phys. 32 (1976) 1591.

[16] C.I Pierre, G Pierre, G. Guelachvili, A Valentin and L Henry, Presented at the Ninth Colloquium on High Resolution Molecular Spectroscopy, Riccione (16–20 September 1985)

[17] A.S. Pine and A G Robiette, J. Mol. Spectry 80 (1980) 388

[18] M. Dubs, D. Harradine, E. Schweitzer, J I. Steinfeld and C. Patterson, J. Chem. Phys. 77 (1982) 3824.

[19] I. Abram, A. de Matrino and R Frey, J Chem Phys 76 (1982) 5727

[20] W Knippers, K. van Helvoort, S Stolte and J. Reuss, Chem. Phys. (1985), to be published

[21] A.R.H. Cole, Table of wavenumbers for the calibration of infrared spectrometers (Pergamon Press, Oxford, 1976).

[22] G Sanna, M. Nardi and M. Bernardini, in Proceedings of the International Conference Laser 1981, ed C B. Collins (STS Press, McLean, 1982) p. 83

[23] E. Borsella et al., to be published

[24] E Bosella, R. Fantoni, G. Petrocelli, G. Sanna, M Capitelli and M. Dilonardo, Chem. Phys 63 (1981) 219

[25] P. Kolodner, C Winterfeld and E Yablonovitch, Opt Commun. 20 (1977) 119

[26] I N Knyazev, N P Kuzmina, V S Letokov, V V Lobko and A A Sarkisyan Appl Phys 22 (1980) 429
[27] M Quack and G Seyfang, Chem. Phys Letters 93 (1982) 442, J Chem Phys 76 (1982) 955
[28] M N R Ashfold, C G Atkins and G Hancock, Chem Phys Letters 80 (1981) 1,
J C Stephenson and D S King, J Chem Phys 78 (1983) 1867
[29] M Quack and E Sutcliffe, Chem Phys Letters 99 (1983) 167
[30] M Quack and E Sutcliffe, Chem Phys Letters 105 (1984) 147
[31] Y Pauleau, D Tonneau and G Auvert, in Laser Processing and Diagnostics, ed D Bauerle, Springer Series in Chemical Physics, Vol 39 (Springer, Berlin, 1984) p 215

ASSIGNMENT OF TWO-PHOTON TRANSITIONS IN SiH_4 (*)

ν_{exp}	$\Delta\nu_{exp}$	$2\nu_{exp}$	ν_{calc}	assignment
936.19	0.28	1872.38	1872.25	36 % $2\nu_4(E)$ 54 % $2\nu_4(F_2)$
			1872.46	42 % $2\nu_4(E)$ 54 % $2\nu_4(F_2)$
936.40	0.16	1872.80	1872.62	50 % $2\nu_4(E)$ 44 % $2\nu_4(F_2)$
			1873.06	44 % $2\nu_4(E)$ 48 % $2\nu_4(F_2)$
947.68	0.23	1895.36	1894.91	98 % $\nu_2+\nu_4$ (F_2)
			1895.71	100 % $\nu_2+\nu_4$ (F_1)
948.78	0.30	1897.56	1897.09	20 % $\nu_2+\nu_4$ (F_1)
				78 % $\nu_2+\nu_4$ (F_2)
950.49	0.33	1900.98	1900.60	66 % $\nu_2+\nu_4$ (F_1)
				30 % $\nu_2+\nu_4$ (F_2)
952.22	0.23	1904.44	1904.71	54 % $2\nu_4(E)$ 42 % $2\nu_4(F_1)$
952.57	0.12	1905.14	1905.06	55 % $2\nu_4(E)$ 42 % $2\nu_4(F_2)$
974.25	0.68	1948.50	1948.88	99 % $2\nu_2(E)$
977.00	0.44	1954.00	1954.34	15 % $(\nu_2+\nu_4)(F_1)$
				61 % $(\nu_2+\nu_4)(F_2)$ 11 % $2\nu_4(F_2)$
			1954.28	85 % $(\nu_2+\nu_4)(F_1)$
				10 % $(\nu_2+\nu_4)(F_2)$

*All frequencies are in cm^{-1}.

Very recently G. Pierre et al [1] have measured the linear absorption spectrum of SiH_4 between 840 and 1040 cm^{-1}. From the analysis of that spectrum they have obtained the effective parameters in the Hamiltonian for the dyades ν_2 and ν_4. Their data have been used to calculate two-photon transitions ($2\nu_2$, $2\nu_4$ and $\nu_2+\nu_4$) which allowed assignment of some multiple photon resonances observed in [2].

[1] G. Pierre, A. Valentin and L. Henry, Can. J. Phys.(in press)
C.I. Pierre and G. Pierre, private communication
[2] M. Snels, R. Larciprete, R. Fantoni, E. Borsella and A. Giardini-Guidoni, Chem. Phys. Lett. 122 (1985) 480

VAN DER WAALS MODES AND ROTATIONAL FINE STRUCTURE IN C_2H_4 DIMERS

M SNELS, R FANTONI [1], M ZEN [2], S STOLTE and J REUSS

Fysisch Laboratorium Katholieke Universiteit Toernooiveld 6525 ED Nijmegen The Netherlands

Received 20 November 1985

IR predissociation spectra for C_2H_4 dimers have been recorded using a cw CO_2 laser as source of radiation and a Ge bolometer as detector Apart from the main peak around 952 cm^{-1} two extra peaks at 916 and 986 3 cm^{-1} have been observed Those two peaks are discussed in terms of van der Waals combination modes and from their relative intensities dimer temperatures in He seeded beams have been obtained Observed peaks show rotational fine structure with a 10 MHz linewidth which implies a predissociation lifetime of 16 ns

1. Introduction

In the last ten years the predissociation of weakly bound van der Waals complexes has been studied both experimentally [1–6] and theoretically [7–12] Since van der Waals bonds are very weak, these clusters can only survive in a very cold and/or collisionless environment which can be obtained in a supersonic expansion of gas through a nozzle In such a molecular beam the clusters formed can consist of two molecules (dimers) or up to many hundreds [13,14], approaching even the situation of a solid-state matrix [15,16] Interaction of a cluster with photons of suitable frequency produces an excited van der Waals complex Since the absorbed energy usually exceeds the bond energy by far, intermolecular relaxation will provoke the rupture of the van der Waals bond In connection with this process a predissociation lifetime is introduced, which represents the lifetime of the excited complex

One of the main problems of studying dimers is the fact that so-called dimer spectra may partially originate from heavier clusters Mass spectra can give some indication about the concentrations of the different species, but since the fragmentation probabilities in the ionizer are not known, they will never give a definite answer about the purity of a dimer spectrum

Bolometric detection suffers from the lack of mass selectivity, but has been shown to be a very sensitive tool to study IR dissociation of clusters [3,4] Moreover, one can use a bolometer in combination with a mass spectrometer, benefiting from the advantages of both

Buck [17] proposed to select different cluster species in a scattering experiment with time-of-flight detection

One of the most studied dimers, $(C_2H_4)_2$, can be considered as an intermediate case between very small clusters (diatomic–rare gas clusters or simple systems like $(N_2)_2$, $(CO_2)_2$, $(N_2O)_2$ and $(C_2H_2)_2$) and larger systems, like $(C_3H_4)_2$ and substituted ethenes In most of these systems some fine structure has been found recently in the dissociation spectra [4,5,19]

The C_2H_4 clusters have been studied extensively by several groups [18–24] using both mass spectrometers [18–23] and bolometer detectors [19,24] For the frequency range around 3000 cm^{-1} a FCL laser [19,24] or a low-resolution OPO [23] has been used, for the 10 μm range CO_2 lasers were employed [18, 20–22] Liu et al [23] suggested some rotational structures, but were not able to resolve these with their low-resolution laser source The results of all those studies were broad absorption bands without any structure, containing contributions of dimers and heavier clusters Since no structure could be measured, the total linewidth has been attributed to

[1] Permanent address ENEA-Dip TIB, C R E., C P 65 00044 Frascati Rome Italy

[2] Permanent address IRST Trento, 38050 Povo (TN) Italy

lifetime broadening [7,20–24], although theory has not provided a relaxation mechanism which could give corresponding predissociation lifetimes of pico seconds

2 Experimental

The molecular beam apparatus is sketched in fig 1. The beam is produced by the supersonic expansion of a mixture of C_2H_4 and He through a 30 μm diameter nozzle into a vacuum chamber which is evacuated by a 1000 ℓ/s oil diffusion pump backed by a 80 m^3/h rotary pump The nozzle temperature can be varied between −50 and 80°C and is stabilized within 0 1°C

A conical skimmer of 600 μm diameter separates the first chamber from the second one which is pumped by a 1000 ℓ/s oil diffusion pump backed by the same 80 m^3/h rotary pump In this chamber the molecular beam is crossed by the radiation from a cw CO_2 laser This laser with a cavity length of 1 95 m can be operated single mode with $^{12}CO_2$, $^{13}CO_2$ and N_2O gas mixtures, providing more than 150 laser lines between 900 and 1050 cm^{-1} The long-time power stability of this laser is better than 1%, the frequency stability better than 1 MHz A piezo-electric translator, mounted on the laser grating, allows a 75 MHz fine tuning of the laser frequency within each single-mode laser line The laser beam is focused to a spot of 0 8 mm diameter on the molecular beam axis

The third chamber which contains the bolometer is pumped by a 3000 ℓ/s oil diffusion pump backed by a 12 m^3/h rotary pump Under typical source conditions, the pressures in the three chambers are $p_1 = 10^{-4}$–10^{-3} Torr, $p_2 = 10^{-6}$–10^{-5} Torr and $p_3 = 10^{-7}$ Torr The distance between laser spot and bolometer is 40 cm In the third chamber the molecules impinge on a doped Ge detector of 1 mm × 1 mm (Infrared Laboratories) on a substrate of sapphire (2 mm × 5 mm) operated at 4.2 K The NEP at 4 2 K is 4 8 × 10^{-13} W $Hz^{-1/2}$, the responsivity 5 × 10^4 V/W and the response time 2 5 ms During the measurements the response time increases due to the so-called cryofrost, which is the condensation of molecules on the cold detector surface The bolometer is well shielded from external sources of heat radiation by screens at temperatures of 77 and 4 2 K and from the laser stray light by several screens between laser and detector

The dissociation spectra were obtained working with a continuous molecular beam and modulating the radiation of the laser The modulated bolometer signal was amplified by a preamplifier (Infrared Laboratories LN-6C) and fed into a lock-in amplifier The lock-in signal has been averaged by microcomputer (Rockwell Aim 65), after subtracting the contribution of the stray light of the laser, i e the laser-induced signal without the presence of the molecular beam

The detection of cluster dissociation by a bolometer has some serious drawbacks One of them is the lack of mass selectivity, another is that the heavier a cluster is the more efficiently its dissociation is detected The third disadvantage is that cryofrost can be a severe problem in using other than very dilute mixtures For this reason we always worked with mixtures containing 2% or 5% C_2H_4 in He In the 5% case our dynamical range was about 3000, i e we can detect an effect 3000 times smaller than our maximum cluster dissociation signal (which is again 1500 times smaller than the total molecular beam signal!) *This huge sensitivity is the main advantage* of the bolometer with respect to a mass spectrometer

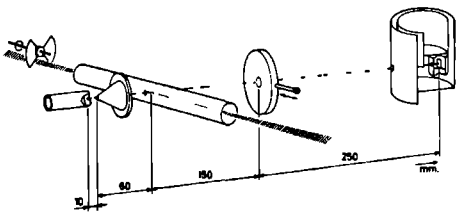

Fig 1. The apparatus

3 Results

Since we want to study the IR predissociation of dimers, we have to minimize the bolometer signal due to laser stray light and absorption of laser radiation by C_2H_4 monomers The stray light was suppressed very efficiently by directing the laser beam through a blackened tube with two 5 mm diameter holes to transmit the molecular beam The bolometer signals were corrected for the very small contribution of

the stray light which remained For all source conditions used, we fortunately observed the total absence of an absorption signal from the C_2H_4 monomer, which is probably due to the fact that the few transitions which lie within the laser bandwidth of 75 MHz start from levels which are hardly populated at the low beam temperatures To check this assumption we measured the absorption of SF_6 for an expansion of 1% SF_6 in He Only a few absorption lines could be observed (near the N_2O laser line R10), which originate from very low lying levels [25]

Using a mass spectrometer, previous IR dissociation measurements in the 10 μm range [18,20,21] showed a tendency for the absorption bands originating from smaller clusters to broaden and shift towards the monomer frequency (949 cm^{-1}), whereas the bigger clusters yield narrower blue-shifted peaks Buck [26] observed in a scattering experiment that C_2H_4 dimers yield a broader absorption band than do bigger clusters. Measurements with pure C_2H_4 (nozzle at 253 K) and with a mixture of 10% C_2H_4 in He (nozzle at 293 K) showed rather narrow (< 12 cm^{-1}) peaks centered at 953 cm^{-1} A 5% C_2H_4 in He mixture expanded through a room-temperature nozzle produced a broader (13 cm^{-1}) structure centered at 952 cm^{-1} This indicates a dominant presence of dimers.

Fig 2 shows three cluster dissociation spectra recorded for a mixture of 5% C_2H_4 in He with a source pressure of 5 atm; the source temperatures were 253 (2a), 293 (2b) and 323 K (2c) Fig 3

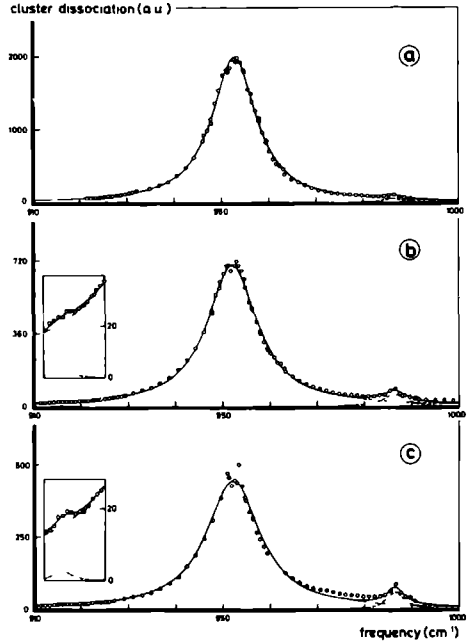

Fig 2 Cluster dissociation spectra for an expansion of a 5% C_2H_4 in He mixture through a 30 μm diameter nozzle Source pressure is 5 atm, nozzle temperatures are 253 (a), 293 (b) and 323 K (c)

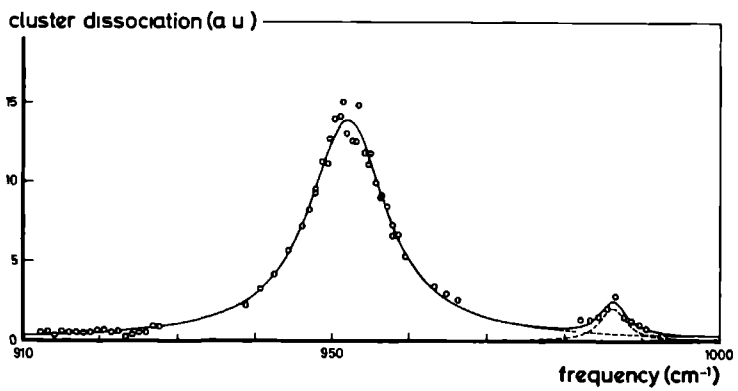

Fig 3 Cluster dissociation spectrum for an expansion of a 2% C_2H_4 in He mixture through a 30 μm diameter nozzle Source pressure is 5 atm, nozzle temperature 293 K

displays the spectrum measured for a mixture of 2% C_2H_4 in He with a source pressure of 5 atm and a source temperature of 293 K The laser power was kept ar 5 W, focused to a spot of 0 8 mm diameter on the molecular beam We checked that up to 20 W the dissociation yield was linear with the laser power In figs 2 and 3 the solid line is the best fit for three Lorentzians through the measured points, the dotted lines represent the three individual Lorentzians An insert shows an enlargement of the section where the smallest peak was found

In the cluster literature [20–22,24] a Lorentzian lineshape has been mainly associated with a homogeneous broadening and a corresponding predissociation lifetime, in the present work we use it because it fits remarkably well the overall predissociation spectrum, without implying homogeneous broadening The positions of the peaks observed in these spectra, their fwhm and relative intensities are listed in table L The intensity of a peak is always the total area under the corresponding Lorentzian curve The reproducibility of the measurements taken around 916 cm^{-1} was within 2% on different days, since this peak in fig 2b is about 10% higher than the wing of the main peak, it is significant Fig 2c takes away any doubts on its presence

The two peaks which are 36 cm^{-1} red-shifted and 34 3 cm^{-1} blue shifted with respect to the main absorption band, are probably due to van der Waals modes in C_2H_4 dimers In the commonly accepted parallel (slightly tilted) dimer configuration [27–29] the out of-plane CH_2 wagging mode of C_2H_4 should couple very strongly with van der Waals stretching or bending modes The coupling of those modes with in-plane fundamental modes of C_2H_4 is expected to be much weaker, which explains the absence of spectral structure due to van der Waals modes in the 3000 cm^{-1} range [19,24]

Our measurements are the first experimental evidence of van der Waals modes in C_2H_4 dimers, whereas for C_2H_4–Ar and C_2H_4–Ne spectral structure has been observed previously [21] From fig 2a we can infer that the peaks at 916 and 986 3 cm^{-1} belong only to the dimers In fact lower beam temperature enhances the production of heavier clusters and increases the signal intensity of the main peak, but leaves the intensity of the other two unchanged Furthermore, measurements on a cooled (253 K) pure C_2H_4 beam have shown only the main peak centered around 953 cm ^{1} (i e the dimer concentration became so low that the van der Waals combination mode was not observed at all) Cooling the nozzle for different seeding mixtures we have always observed a narrowing of the main peak with a small blue-shift of the maximum (≈ 1 cm^{-1}), together with a relative decrease in intensity of the two satellites All these features confirm that data reported in fig 2 are essentially due to dimers

The van der Waals bond in the C_2H_4 dimer has been described by a potential well with a depth of about 350 cm^{-1} and a bond distance of about 4 Å [27–29] From our measurements we find a van der Waals frequency ν_{vdW} of about 36 cm^{-1} (952 – 916 cm^{-1}) If one assumes a Boltzmann distribution over the vi-

Table 1
The positions of the peaks (cm^{-1}), the full widths at half-maximum height (cm^{-1}), and relative intensities (%) of the spectra in figs 2 and 3

	Fig 2a	Fig 2b	Fig 2c	Fig 3
nozzle temperature (K)	253	293	323	293
position peak A		916	916	
position peak B	952 6	952 0	952 1	951 8
position peak C	986 2	986 4	986 4	986 2
fwhm peak A		5 5	4 5	
fwhm peak B	11 4	12 9	13 8	12 3
fwhm peak C	5	5 5	4 5	4 1
ratio C/B	1 1	3 5	4 4	4 8
ratio A/C		3 3	4 4	
max signal (au)	20	7 0	4 4	2 1

brational levels in the van der Waals well, the population of the level v follows from $P(v) = \exp(-36v/kT_d)$ A dimer temperature T_d fits the ratio of the intensities measured at $\nu = \nu_D - \nu_{vdW}$ and $\nu = \nu_D + \nu_{vdW}$, with $\nu_D = 952\ cm^{-1}$ the center frequency of the main peak We assume equal transition strengths for both transitions For a nozzle temperature T_0 of 293 K (fig 2b) one finds $T_d = 15\ 2 \pm 0\ 8$ K, for $T_0 = 323$ K (fig 2c) one has $T_d = 16\ 6 \pm 0\ 3$ K, in case of 5% C_2H_4 in He The temperature of the dimers is higher than the monomer temperature (about 7 K) under these beam conditions, since some of the heat of dimerization will remain as rotational and vibrational energy in the dimer The number of collisions with the monomer is too small to provide a sufficient relaxation to the local translational temperature [30], and in addition He is not very effective in vibrational relaxation Once the observed peaks are assigned as difference and sum combinations of a dimer excitation ν_D with a van der Waals mode ν_{vdW}, the peak found at 916 cm^{-1} yields the value of the van der Waals frequency itself while from the position of the peak at 986 3 cm^{-1} we can deduce the cross anharmonicity constant $\chi_{D\,vdW}$ From 986 3 $cm^{-1} = \nu_D + \nu_{vdW} + \chi_{D,vdW}$ follows $\chi_{D,vdW} = -1\ 7\ cm^{-1}$ This implies that there should be a hot band on the red shoulder of the main peak, around 950 3 cm^{-1} Such a hot band is seen in fig 2c, it is less evident in fig 2b and is not at all present in the cold spectrum in fig 2a The other structures at the top (952 cm^{-1}) can be due to hot bands of other van der Waals modes or to rotational fine structure of the dimer This point is further discussed below

We also tried to find the overtone of the van der Waals mode, $\nu_D + 2\nu_{vdW}$, which is expected to have an intensity of 0 2% of the main peak A very broad peak (fwhm = 25 cm^{-1}) was indeed found around 1020 cm^{-1} in measurements performed on the 5% C_2H_4 mixture This peak seems too strong and too broad to be exclusively identified as the combination of ν_D with the second harmonic of the van der Waals mode at 36 cm^{-1} Perhaps this peak at 1020 cm^{-1} originates from another van der Waals combination with ν_D, yielding $\nu'_{vdW} \approx 68\ cm^{-1}$ (neglecting the unknown cross anharmonicity constant of this mode $\nu'_{vdW} + \nu_D$)

As can be noticed in table 1 the widths for the van der Waals combinations have a very peculiar behaviour with respect to the main dimer peak at 952 cm^{-1} We assume that the width of the ν_D peak is due to the internal degrees of freedom of the dimer, which is confirmed by the comparison between fig 2b and fig 3 Under the same source conditions the most diluted mixture is the coldest, yielding a narrower width for the main absorption peak, while the ratio in intensity of the van der Waals combinations with the former is unchanged In the dimer the coupling of the ν_D mode to the van der Waals modes depends on the configuration of the complex This means that the width of the van der Waals peaks in the spectrum reflects the coupling probabilities with the ν_D In fact sum and difference combinations with $\nu_{vdW} = 36\ cm^{-1}$ show the same narrow width (fwhm = 4 5 cm^{-1}), whereas a complete different width for the $\nu'_{vdW} \approx 68\ cm^{-1}$ mode could reflect a different intramolecular coupling

During the measurements we were puzzled because the measured points near the top of the dimer peak (ν_D) seemed to deviate reproducibly from the Lorentzian while the points in the wings behaved

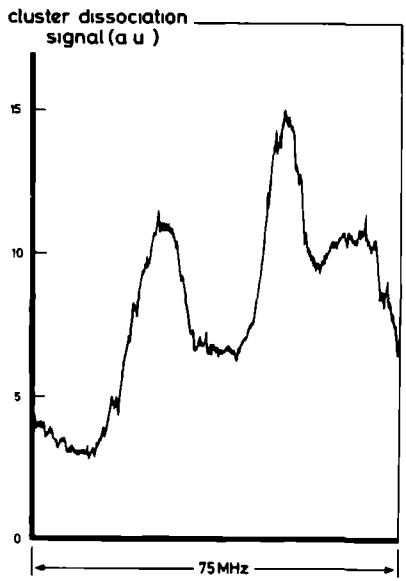

Fig 4 Cluster dissociation signal on laser line 10 μm R38 with a laser power of 5 W Scan over 75 MHz

remarkably well Furthermore the point measured with the 10 μm R38 line of the CO_2 laser (986 57 cm^{-1}) near the top of the van der Waals peak $\nu_D + \nu_{vdW}$ reproduced very badly Within the FSR of our laser a scan with the piezo-electric translator has been performed yielding a tuning range of 75 MHz for each laser line For some laser lines we found two or three peaks (fwhm $\approx$ 10 MHz) within the 75 MHz scan Fig 4 shows the result of a scan on 10R38 Similar results were found on 10R36 and 10R40 On the main peak only 10P10 and 10P12 showed comparable structure, but less pronounced Other laser lines showed no structure at all The observed linewidth of the rotational fine structure of 10 MHz gives us a lower limit for the predissociation lifetime of 16 ns This value agrees rather well with the upper limit of 10 ns suggested recently by Mitchell et al [31] The relative intensity of the observed fine structures does depend on the beam temperature, whereas the position of the peaks does not This observation suggests that we are really dealing with rotational fine structure At this moment the small frequency range investigated (75 MHz on each laser line) does not allow us to give a satisfactory interpretation of the structure To obtain more information we shall employ a wave-guide laser with a FSR of 300 MHz

An investigation around 3000 cm^{-1} (in-plane vibrations of C_2H_4) did not show any structure, although the resolution of the FCL laser should be sufficient to find structures similar to ours [19,24] The presence of fine structure may depend on the coupling between the excited mode and the van der Waals modes This will be a subject of further investigation

Acknowledgement

The authors gratefully acknowledge the specialist help of C Liedenbaum in preparing the bolometer R Sanders is thanked for his enthusiastic cooperation during the measurements We thank Dr. H. Bluyssen and A van Etteger who designed our CO_2 laser The technical assistance of C Sikkens and F van Rijn is also appreciated One of us (RF) thanks ZWO (Netherlands Organisation for the Advancement of Pure Research) for a fellowship

References

[1] D S Bomse, J B Cross and J J Valentini, J Chem Phys 78 (1983) 7175
[2] J Geraerdts, S Stolte and J Reuss, Z Physik A304 (1982) 167,
J Geraedts, M Snels, S Stolte and J Reuss, Chem Phys Letters 106 (1984) 377
[3] R E Miller, R O Watts and A Ding, Chem Phys 83 (1984) 155
[4] R F Miller and R O Watts, Chem Phys Letters 105 (1984) 409,
R E Miller, P F Vohralik and R O Watts, J Chem Phys 80 (1984) 5453,
G Fischer, R E Miller and R O Watts, J Phys Chem 88 (1984) 1120
[5] C A Long, G Henderson and G E Ewing, Chem Phys 2 (1973) 485
[6] T E Gough, R E Miller and G Scoles, J Chem Phys 69 (1978) 1588, J Phys Chem 85 (1981) 4041
[7] G E Ewing, J Chem Phys 71 (1979) 3143, 72 (1980) 2096, Chem Phys 29 (1978) 253
[8] W Klemperer, Faraday Discussions Chem Soc 73 (1982) 115
[9] J A Beswick and J Jortner, J Chem Phys 68 (1978) 2277, 73 (1980) 3653
[10] J M Hutson, D C Clary and J A Beswick, J Chem Phys 81 (1984) 4474
[11] M Snels, J Geraedts, S Stolte and J Reuss, Chem Phys 94 (1985) 1
[12] G Brocks and A van der Avoird, Mol Phys 55 (1985) 1L
[13] O Echt, K Sattler and E Recknagel, Phys Letters 90A (1982) 185
[14] T E Gough, D G Knight and G Scoles, Chem Phys Letters 97 (1983) 155
[15] W J Wiesenhahn, G Bischoff and J M D'Auria, Nucl Instr Meth 124 (1975) 221
[16] J M Zellweger, J M Philippoz, P Melinon, R Monot and H van den Bergh, Phys Rev Letters 52 (1984) 522
[17] U Buck and H Meyer, Phys Rev Letters 52 (1984) 109
[18] J Gereadts, Ph D Thesis, Katholic University of Nijmegen (1983).
[19] G Fischer, R E Miller and R O Watts, Chem Phys 80 (1983) 147
[20] M P Casassa, D S Bomse, J L Beauchamp and K C Janda, J Chem Phys 72 (1980) 6805,
M P Casassa, D S Bomse and K C Janda, J Chem Phys 74 (1981) 5044,
C M Western, M P Casassa and K C Janda, J Chem Phys 80 (1984) 4781
[21] M P Casassa, C M Western and K C Janda, J Chem Phys 81 (1984) 4950
[22] M Hoffbauer, K Liu, C Giese and W Gentry, J Chem Phys 78 (1983) 5567

[23] W Liu, L K Kolenbrander and J M Lisy, Chem. Phys Letters 112 (1984) 585
[24] G Fischer, R E Miller, P F Vohralik and R O Watts, J Chem Phys 83 (1985) 1471
[25] S Avrillier, J -M Raymond, Ch J Bordé, D Bassi and G Scoles, Opt Commun 39 (1981) 311
[26] U Buck, private communication.
[27] A van der Avoird, P Wormer, F Mulder and J Berns, Topics Current Chem 93 (1980) 1.
[28] E Padma Malar and A Chandra, J Phys Chem 85 (1981) 2190
[29] K Suzuki and K Iguchi, J Chem Phys 77 (1982) 4594
[30] L S Bernstein and C E Kolb, J Chem Phys 71 (1979) 2818
[31] A Mitchell, M J McAuliffe, C F Giese and W R Gentry, J Chem Phys 83 (1985) 4271.

CHAPTER 3

IR DISSOCIATION OF AMMONIA CLUSTERS

M. SNELS, R. FANTONI*, R. SANDERS AND W. LEO MEERTS

Fysisch Laboratorium, Katholieke Universiteit
Toernooiveld 6525 ED Nijmegen, The Netherlands

ABSTRACT

Dissociation spectra of NH_3 clusters have been recorded using a CW CO_2 laser. For the dimer two absorption bands have been found at 979 cm^{-1} and 1004 cm^{-1}, which originate from the excitation of two non-equivalent NH_3 molecules. A tunneling motion is held responsible for the observed structure on one of these bands. Heavier NH_3 clusters dissociate at frequencies between 1020 cm^{-1} and 1100 cm^{-1}. The dissociation spectrum of the SiH_4-NH_3 complex shows one peak centered at 972.3 cm^{-1}.

*Permanent adress : ENEA-Dip. TIB, C.R.E., C.P. 65, 00044 Frascati, Roma, Italy

Recently several hydrogen-bonded complexes have been investigated using various experimental methods Klemperer and coworkers used microwave and infrared spectroscopic techniques to examine a series of complexes containing NH_3 produced in a molecular beam [1] Pine et al studied the dissociation spectra of $(HF)_2$ and $(HCl)_2$ in a static gas cell using a tunable difference-frequency laser [2] Equilibrium structures for some complexes could be established and valuable information on the internal motions have been obtained Dissociation energies have been found which are usually smaller than predicted by ab initio calculations [3]. In particular the ammonia dimer was not expected to dissociate upon excitation with a single 10 6 μm photon

Experiments showed [1,4] that one 970 cm^{-1} photon was sufficient to cause dissociation of this complex Howard et al [4] studied the IR dissociation of $(NH_3)_n$ complexes. Their spectra show a single broad peak at 977.2 cm^{-1} corresponding to the dimer dissociation and structures due to heavier clusters between 1020 cm^{-1} and 1060 cm^{-1} A molecular beam electric deflection study [6] demonstrated that the NH_3 dimer has a permanent electric dipole moment. Fraser et al [1] measured the dipole moment along the dimer axis (0 74 D), moreover, they found two peaks between 970 cm^{-1} and 985 cm^{-1} which showed a different behaviour in their IR-microwave double resonance measurements. In a very recent work [5] they suggest that the two peaks correspond with two torsional sublevels of the complex.

Investigations of NH_3 complexes in CO [7] and N_2 [8] matrices demonstrated the existence of two dimer bands of nearly the same intensity separated by 12 cm^{-1} (CO) and 17.5 cm^{-1} (N_2), respectively. This suggests that there might be also two well separated bands for NH_3 dimers produced in a molecular beam. Indeed we observed two broad bands (FWHM = 14 cm^{-1}) in the $(NH_3)_2$ dissociation spectrum centered at 979 cm^{-1} and 1004 cm^{-1}. A structure richer than seen by Fraser et al [1] emerged in the first band. Dissociation of heavier clusters occurred at frequencies between 1020 cm^{-1} and 1100 cm^{-1}, which agrees with the results of [4] and matrix spectra [8].

In the next section the experimental apparatus is described briefly. Subsequently a discussion of the measured spectra is presented.

EXPERIMENTAL APPARATUS

Since the molecular beam apparatus has been discussed before [9], only a short description follows The beam is produced by supersonic expansion of a mixture of NH_3 in He through a 30 μm nozzle into a vacuum chamber For the reported spectra the stagnation pressure was 5 atm The temperature of the nozzle can be varied between -50 °C and 150 °C and is stabilized within 0 1 °C A conical skimmer separates the first chamber from the second which is independently pumped In this chamber the molecular beam is crossed by the radiation from a CW CO_2 laser This laser with a cavity length of 1 95 m can be operated single- mode with $^{13}CO_2$, $^{12}CO_2$ and N_2O gasmixtures, providing more than 250 laserlines between 880 cm^{-1} and 1100 cm^{-1} A piezo electric translator, mounted on the laser grating, allows a 75 MHz fine tuning of the laser frequency within each laser line The gaussian laser beam is focussed to a spot of 0 8 mm diameter on the molecular beam axis The laser power in all the present experiments was 5 Watt. The molecular beam is detected by a Ge bolometer (Infrared Laboratories) operated at 4 2 K This very sensitive device is located in a third vacuum chamber, 400 mm from the interaction point

The dissociation spectra were obtained working with a continuous molecular beam and modulating the radiation of the laser The modulated bolometer signal was preamplified, fed into a lock-in amplifier and averaged by a microcomputer The reproducability of the observed spectra was better than 5 %

RESULTS

$(NH_3)_n$

A mixture of 2 % NH_3 in He was expanded from a 294 K nozzle The dissociation spectrum is displayed in fig 1b and shows two absorption bands of comparable intensity centered at 979 cm^{-1} and 1004 cm^{-1} The two peaks in the first band, at 977 2 cm^{-1} and 980 9 cm^{-1}, correspond to those measured by Fraser et al [1], the second band has never been observed before Fig 1a displays a spectrum for a nozzle temperature of 248 K, with the other beam conditions unchanged The two bands which are due to dimer dissociation remain, but new structures between 1020 cm^{-1} and 1100 cm^{-1} appear As already discussed by Howard et al [4] those correspond to the dissociation of heavier clusters Pimentel et al observed $(NH_3)_n$ - complexes (n>2) in a N_2 matrix [8] at frequencies

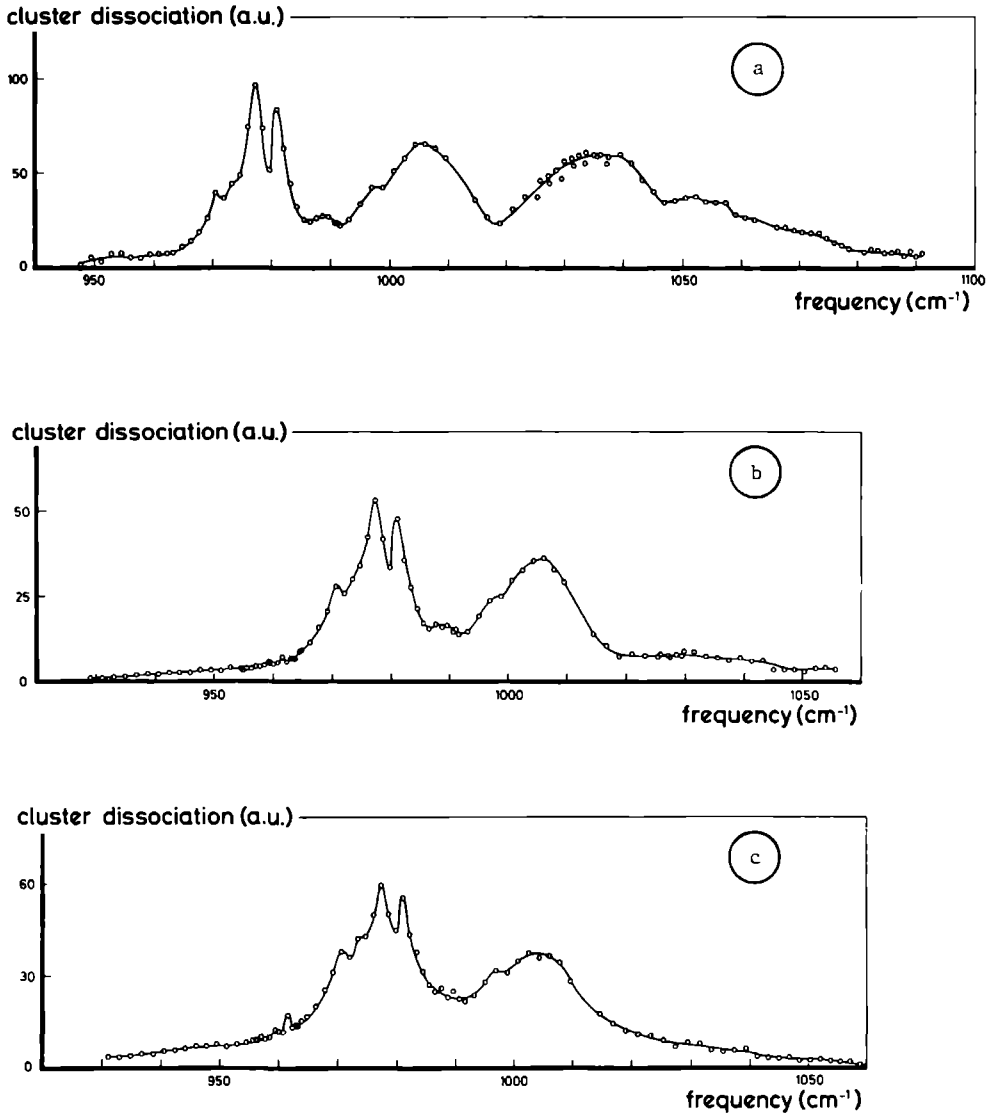

Fig.1 a,b) Cluster spectrum for 2% NH_3 in He, nozzle temperature 248 K (a), 294 K (b)

c) Cluster spectrum for 5% NH_3 in He, nozzle temperature 423 K

from 1015 to 1065 cm^{-1}. Varying the nozzle temperature from room temperature to 150°C we noticed that the dimer signal decreased only a factor of two, whereas for dimers of SF_6, SiF_4 and SiH_4 a very drastic dependence has been observed [10]. This observation suggests that the dimer bond in $(NH_3)_2$ is much stronger than in the other complexes.

Additional evidence for a rather strong NH_3 dimer bond has been given by Buck et al. [19]. In a scattering experiment with a secondary He beam an energy of 520 cm^{-1} was transferred to NH_3 dimers without causing their dissociation. This gives a lower limit of 520 cm^{-1} to the binding energy of $(NH_3)_2$, the upper limit is 970 cm^{-1}.

For very cold beam conditions (fig. 1a) a broad band is observed, which corresponds to heavier clusters. This broad band consists of a few bands which emerge one by one, when the beam temperature is varied. Apparently trimers and tetramers give rise to different spectral structure. Peculiar of the cluster spectra of NH_3 is that dimers and heavier clusters produce well separated absorption bands.

A third spectrum (fig. 1c) has been recorded for 5 % NH_3 in He at a nozzle temperature of 423 K. This spectrum shows a few extra peaks and a broadening of the two dimer bands. Since the two bands in fig. 1b show the same behaviour when we change the beam conditions (their relative strength does not change), both must be due to the same cluster species, which is shown to be the NH_3 dimer [1,4,8].

In order to understand the origin of the two dimer bands we have to consider the structure of the $(NH_3)_2$ complex. Microwave experiments [5] on several isotopic species of $(NH_3)_2$ have provided constraints on the dimer structure. Six parameters are sufficient to describe the dimer geometry (fig. 2). Three of them, the distance between the centers of mass of the two molecules, R, and the two angles θ_1 and θ_2 have been fixed by the microwave results (θ_1 and θ_2 are the angles between the dimer axis and the C_{3v} axis of molecule 1 and 2 respectively, χ_1 and χ_2 stand for the rotation of the two molecules around their C_{3v} axes and ϕ for the rotation of molecule 2 around the dimer axis). The structure suggested by Nelson et al. [5] (θ_1=48.6° ,θ_2=115.5°, χ_1=0°, χ_2=180°, ϕ=0° and R=3.3374 Å) will be taken as a starting point for our discussion.

This structure for the NH_3 dimer contains two non-equivalent molecules ; one of them (2) is mainly a hydrogen donor , the other (1) a hydrogen acceptor. The same nomenclature has been used as for the dimers of HF and HCl [2].

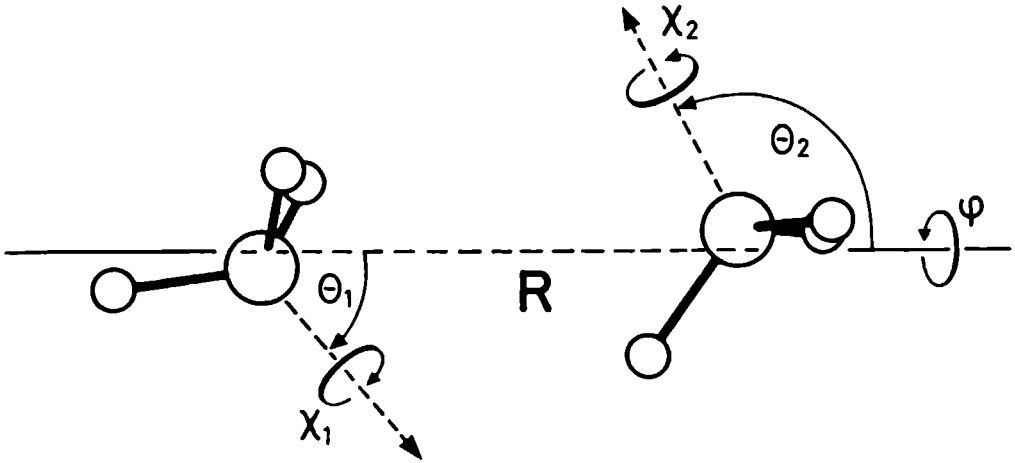

Fig 2 NH_3 dimer, structure according to Nelson et al [5]

It has been suggested [4] that inversion of the NH_3 molecule in the dimer might occur, but in the microwave experiments on $(NH_3)_2$ [5] no transitions related to (hindered) inversion have been observed A study of complexes of NH_3 with other molecules (HCN, OCS, CO_2, N_2O and HCCH) [1] has not given any evidence for this inversion either Since the hydrogen bond in these complexes is surely weaker than in the ammonia dimer we do not expect inversion to occur in the latter The structure which has been proposed by Fraser et al produces a very high barrier for inversion In the structure with a linear N-H--N bond, however, which is the result of several Hartree Fock calculations [15], inversion seems to be possible for the hydrogen donor

Since a strong effect of the resonant dipole-dipole interaction in excited dimers of SF_6 and other high symmetry molecules has been observed [10,11], it is worthwhile to calculate the magnitude of this interaction in the ammonia dimer The ν_2 vibration of NH_3 is a non-degenerate mode, whose transition dipole moment $\mu_{01} = 0\ 24\ D$ [14]

The resonant dipole-dipole term in the Hamiltonian is

$$H_{dd} = \mu_{01}^2/(4\pi\varepsilon_0 R^3) \cdot (\cos(\theta_1+\theta_2)-3\cos\theta_1\cos\theta_2)$$

For θ_1= 48.6°,θ_2= 115.5° and R=3.3374 Å , H_{dd} takes the value -0.83 cm^{-1}. This value is negligible in comparison with a splitting of 25 cm^{-1} between the two dimer bands at 979 and 1004 cm^{-1}. Considering H_{dd} as a perturbation of two levels which are already 25 cm^{-1} spaced, the additional shift is less than 0.1 cm^{-1}.

Since we ruled out the possibility of inversion and calculated the negligible effect of resonant dipole-dipole interaction, we can conclude that the two bands in the dimer spectrum originate from the excitation of the two non-equivalent NH_3 molecules in the dimer. Similarly the two dimer bands observed in matrix experiments [7,8] were explained as excitation of two non-equivalent molecules which, however, were assumed to form a complex with a linear N-H--N hydrogen bond. Hartree-Fock calculations yield, for the geometry θ_1=100.9°, θ_2=153.4°, χ_1=180°, χ_2=0°,ϕ=0° and R=3.3672 Å, obtained in [16],two dimer vibrations for each fundamental vibration of NH_3. Since the Hartree-Fock calculations [16] yield monomer absorption frequencies which are about 20 % too high, we scaled all the reported frequencies down by 20 %. The dimer frequencies corresponding to the ν_2 (umbrella) mode of the NH_3 molecules are separated by 7 cm^{-1} (after scaling).

Assuming the structure proposed by Nelson et al., the excitation of the ν_2 (umbrella) mode in two non-equivalent NH_3 molecules in the dimer produces two different dimer vibrations. Since no Hartree-Fock calculations are available for Nelson's structure we tried to calculate the separation between the two dimer-vibrations using a simple model. In first approximation we substitute the two NH_3 molecules in the dimer by two dipole moments, which are different for ground- and excited state [12]. The difference in dipole-dipole energy between the ground- and excited state of the dimer amounts to

$$\Delta E = (4\pi\varepsilon_0) \cdot(\mu_g(\mu_e-\mu_g)/R^3)\cdot (3\cos\theta_1\cos\theta_2-\cos(\theta_1+\theta_2)) \qquad (1)$$

where μ_g and μ_e are the permanent dipole moments of ground- and excited state of the NH_3 monomer,respectively. According to eq.(1) the excitation of either of the NH_3 molecules in the dimer yields the same value for ΔE (=4.76 cm^{-1}), thus

there is no splitting. But this equation is only valid for ideal dipoles, i.e. point dipoles. Certainly it is not valid for physical dipoles (N-H = 1.01 Å) at a short distance (R=3.3374 Å). In the latter case we have to modify the model and assume a charge distribution for the monomer (in ground- and excited state) and calculate the total electrostatic energy of one of the NH_3 molecules, in the electric field produced by the other NH_3.

By IR high resolution measurements Shimoda et al. [12] obtained dipole moments μ_g and μ_e as well as accurate values for the rotational constants. We determined the positions of N and H atoms in the NH_3 molecule in ground- and excited state from these rotational constants. In order to match the observed dipole moments we put appropriate charges of q on each H-atom and -3q on the N-atom. The coordinates of the NH_3 molecule and the corresponding charge q for ground- and excited state are given in table 1. Even the quadrupole-moment calculated for this charge distribution agrees rather well with the observed [13]. The dimer is built up from two NH_3 molecules, whose relative orientations are fixed by the six parameters given in [5]. We assume that the NH distances and HNH angles in each molecule in the complex are the same as in the monomer. The coordinates of the eight atoms of the dimer in the vibrational ground state are listed in table 2.

The electrostatic energy has been calculated for groundstate (E_0) and for two different excited states of the dimer (E_1 and E_2). We find E_1-E_0= 29.6 cm^{-1} and E_2-E_0 = 19.6 cm^{-1}. Our simple model yields a splitting of 10 cm^{-1} ; the peak corresponding to the excitation of molecule (1), the hydrogen acceptor, is blue shifted with respect to the peak corresponding to the excitation of the hydrogen donor (2). Note that both dimer-frequencies are blue-shifted with respect to the frequency of the monomer vibration.

The preceding discussion explains the observation of two dimer bands. Now we want to find an explanation for their different spectral appearance. The band at 979 cm^{-1} is very structured, the other band (at 1004 cm^{-1}) looks very smooth. Furthermore, figure 1 shows that increasing the nozzle temperature produces new peaks around 961.5 and 973.3 cm^{-1}. In addition, cooling the nozzle narrows the bands. This observation suggests that the width of the two dimer bands is determined by internal degrees of freedom, which become depopulated for colder beams. In their microwave experiments Nelson et al [5] observed two vibrational states α and β, whose rotational constants B+C differ by 300 kHz. Double resonance experiments [1] showed that the two peaks at 977.2 and 980.9 cm^{-1}

Table 1

Coordinates of the atoms of the ammonia molecule for ground- and excited (ν_2) state, respectively. Charges of q were put on each H-atom and -3q on the N-atom, in order to match the experimentally observed dipole moments [12]. For this charge distribution a quadrupole moment has been calculated (Q_{calc}).

Ground state

H1	H2	H3	N
-0.47335	-0.47335	0.94670	0.00000
-0.81986	0.81986	0.00000	0.00000
-0.30439	-0.30439	-0.30439	0.06523

μ_g = 1.47147 D
B_g = 9.9442 cm^{-1}
C_g = 6.2204 cm^{-1}
q = 0.2763 e
Q_{calc} = -2.48 DÅ
Q_{exp} = -2.12 DÅ

Excited state

H1	H2	H3	N
-0.47745	-0.47745	0.95491	0.00000
-0.82697	0.82697	0.00000	0.00000
-0.29079	-0.29079	-0.29079	0.06231

μ_e = 1.2480 D
B_e = 9.9802 cm^{-1}
C_e = 6.1139 cm^{-1}
q = 0.2453 e
Q_{calc} = -2.34 DÅ

Table 2

Coordinates of the atoms in the vibrational ground state of the dimer, assuming the structure proposed by Nelson et al. [5].

H1	H2	H3	N1	H4	H5	H6	N2
0.5414	0.5414	-0.3977	-0.0489	-0.0710	-0.0710	-0.6823	0.0589
-0.8199	0.8199	0.0000	0.0000	0.8199	-0.8199	0.0000	0.0000
-1.5149	-1.5149	-2.5801	-1.6256	2.2270	2.2270	0.9453	1.6406

Rotational constants: A = 125.729 GHz
B = 5.118 GHz
C = 5.046 GHz

correspond to α and β In [5] it was suggested that those states are two torsional sublevels of the NH_3 dimer, from the difference in rotational constant -assuming a threefold barrier for internal rotation- a barrier height of 700 cm^{-1} is calculated, as well as an energy difference of 400 MHz between the two torsional sublevels This hypothesis does not explain the double resonance results Changing the barrier to internal rotation by 10 or 20 % for the excited NH_3 complex, we calculated (following the treatment of [5]) that the resulting splittings for the torsional states in the vibrationally excited dimer do not exceed a few GHz, whereas the two peaks observed in the IR absorption differ by about 3 7 cm^{-1}

In order to explain the observed structures we suggest that the NH_3 dimer exhibits a tunneling motion as observed in HF dimers Starting from the structure in fig 2 with θ_1=48 6° ,θ_2=115 5°, χ_1=0°, χ_2=180°, ϕ=0° and R=3 3374 Å, we can obtain an equivalent situation changing slightly θ_1, θ_2, χ_1 and χ_2 to θ_1= 64 5°, θ_2=131 4°, χ_1=60° and χ_2=120° The barrier for this tunneling motion should be rather low Such a tunneling barrier causes a splitting of the levels in the groundstate (ΔE_0) and in general different splittings ΔE_a and ΔE_b for the vibrational excited states ν_a (1004 cm^{-1}) and ν_b (979 cm^{-1}) The selection rules for infrared transitions in the dimer [2,17] yield transitions ν_a^+, ν_a^-, ν_b^+ and ν_b^- with $\nu_a^+-\nu_a^- = \Delta E_a-\Delta E_0$ and $\nu_b^+-\nu_b^- = \Delta E_b+\Delta E_0$ (fig 3) Our simple model using only the electrostatic energy of point charges, yields barrier heights of 75.3 cm^{-1} (groundstate), 72 8 cm^{-1} (ν_a) and 62 8 cm^{-1} (ν_b) Slightly different barriers are expected to originate comparable splittings

Considering the dimer as a near prolate symmetric top (A≈125 GHz, B≈C≈5 GHz),the energy levels for the vibrational ground state can be approximated by

$$E_0(\tau,J,K) = E(\tau) + BJ(J+1) + K^2(A-B) \pm \tfrac{1}{2}\Delta E_0(\tau,J,K)$$

and for the vibrationally excited states by

$$E_{a,b}(\tau,J,K) = E(\tau) + BJ(J+1) + K^2(A-B) \pm \tfrac{1}{2}\Delta E_{a,b}(\tau,J,K)$$

where $E(\tau)$ is the energy due to the tunneling mode, and ΔE_0 and $\Delta E_{a,b}$ are the splittings caused by the tunneling barrier The rotational quantum numbers for the dimer are denoted by J and K, rotational constants A,B and C are considered to be the same for ground- and excited states For a beam temperature of 10 to

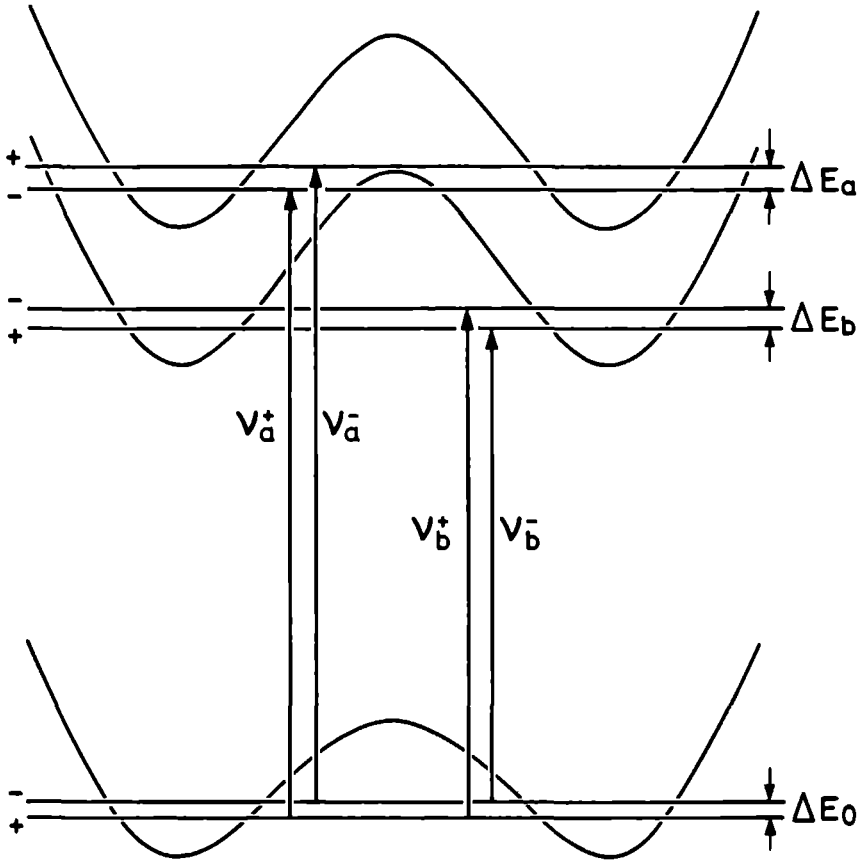

Fig.3 IR transitions for the NH_3 dimer, in the presence of a tunneling barrier

20 K one finds that mainly the K = 0,±1,±2 states are populated Furthermore we assume that the tunneling mode is not excited The relatively small value of B (=0.17 cm^{-1}) prevents the observation -in our experiment- of J-resolved ΔK = 0,±1 transitions. The J-manifolds only cause an effective broadening of the ΔK = 0,±1 transitions In our dimer geometry-the transitions involving ν_a and ν_b both form hybrid bands, ν_b however, is mainly a perpendicular band ($\mu_\perp^2$ $\mu_\parallel^2$ = 80 . 20) and the ΔK = ±1, ΔJ =0,±1 transitions should be dominant. For the ν_a band we find that $\mu_\perp^2 : \mu_\parallel^2$ = 57 . 43. Therefore we assume that the two most important features in the ν_b band are corresponding to the K = 0 → 1 doublet. This assumption yields a band origin for ν_b of about 975 cm^{-1}. We can make a tentative assignment of the rest of the spectrum One peak of the K=1→0 doublet corresponds to the R12 laserline (970.5 cm^{-1}), and the K=1→2 doublet is responsible for the intensity around 987 cm^{-1}. For a higher beam temperature the population of the K=2 level increases and the K=2→2 and K=2→1 transitions appear, the peak at the N_2O line R28 (961.5 cm^{-1}) and the shoulder at R16 (973.3 cm^{-1}) emerge in the spectrum of fig 1c. In table 3 the transitions predicted by our tentative assignment are listed. A beam temperature of 10-15 K could be estimated from the observed spectral width of the ν_b band.

Since the tunneling doublets in the ν_a band are determined by the difference in splittings of ground- and excited state, which are smaller than 1 cm^{-1}, we do not resolve them. This tentative assignment can be tested in microwave experiments using frequencies between 50 and 100 GHz, in order to measure the tunneling splittings in the vibrational ground state.

Table 3

Transitions in the ν_b band (tentative assignment)

K → K'		
0 → 0	973.5 cm^{-1}	976.5 cm^{-1}
1 → 1	972.9 cm^{-1}	977 1 cm^{-1}
2 → 2	971.8 cm^{-1}	978.2 cm^{-1}
0 → 1	977.2 cm^{-1}	980.8 cm^{-1}
1 → 2	984.4 cm^{-1}	989.6 cm^{-1}
2 → 3	991.0 cm^{-1}	999.0 cm^{-1}
1 → 0	969.2 cm^{-1}	972.8 cm^{-1}
2 → 1	960.3 cm^{-1}	965.7 cm^{-1}

SiH_4-NH_3

Mixed clusters containing NH_3 have been investigated both experimentally [1] and theoretically [18]. No information was available on the SiH_4-NH_3 system. The hydrogen bond in this complex can only be formed between an H-atom of SiH_4 and the lone pair of NH_3.

We expanded a mixture of 1 % NH_3, 1 % SiH_4 in He through a 30 μm nozzle at room temperature. The spectral region between 880 and 1020 cm^{-1} has been investigated. Because the bolometer is not mass-selective, several different clusters may contribute to the spectrum. Contributions due to $(NH_3)_2$ and $(SiH_4)_2$ were subtracted after normalization. The SiH_4 dimer spectrum has been taken from [10]. After subtraction of the other contributions only one single peak at 972.3 cm^{-1}, due to the mixed cluster SiH_4-NH_3, remained (fig 4). Since the ν_2 vibration in SiH_4 (970.9 cm^{-1}) is only very weakly allowed, the observed peak must be due to excitation of the strong ν_2 (umbrella) vibration in the NH_3 molecule. The blue shift of the observed structure with respect to the NH_3 monomer frequency is comparable to that in other NH_3 complexes [1]. A spectral feature corresponding to the excitation of the ν_4 mode in SiH_4 has not been found. This implies that such a peak was too narrow or too broad to be distinghuished from the SiH_4 dimer spectrum.

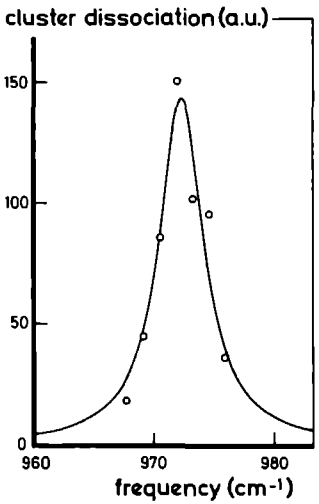

Fig.4 Dissociation spectrum for 1% SiH_4, 1% NH_3 in He, nozzle at room temperature, after subtracting the contributions of $(SiH_4)_2$ and $(NH_3)_2$. Error bar is ± 30 a.u for each point.

CONCLUSIONS

In the IR dissociation spectra of the NH_3 dimer a second band has been observed. The two dimer bands are due to two different dimer vibrations, which correspond to non-equivalent NH_3 molecules in the dimer The spectral structure can be explained in terms of a tunneling motion A tentative assignment of the main features in the spectra yields tunneling splittings of 1 5 - 3 cm^{-1} for the ground state of the dimer More detailed information can be obtained in microwave experiments, using frequencies between 50 and 100 GHz It would be also very interesting to measure the dimer bands in the 3μm region, where higher resolution sources are available. Since the NH_3 dimer bond energy is comparable to that of the HCl dimer, their spectra might be obtained using a cooled cell

ACKNOWLEDGEMENTS

Authors gratefully acknowledge the specialist help of Dr M Zen and C. Liedenbaum in preparing the bolometer.
We thank Dr. H Bluyssen and A. van Etteger who designed our CO_2 laser. The technical assistance of C Sikkens and F. Van Rijn is also appreciated.
Discussions with Prof. J. Reuss and Dr. S. Stolte are greatly appreciated.

One of us (R.F) thanks Z W.O (Netherlands Organisation for the Advancement of Pure Research) for a fellowship

REFERENCES

[1] G.T. Fraser, D.D. Nelson Jr.,A. Charo and W. Klemperer, J. Chem. Phys. 82 (1985) 25351

[2] A.S. Pine, W.J. Lafferty and B.J. Howard, J. Chem. Phys. 81 (1984) 2939
N. Ohashi and A.S. Pine, J. Chem Phys. 81 (1984) 73

[3] Z. Latajka and S. Scheiner, J. Chem. Phys. 84 (1986) 341

[4] M.J. Howard, S. Burdenski, C.F. Giese and W.R. Gentry, J. Chem. Phys. 80 (1984) 4137

[5] D.D. Nelson Jr.,G.T. Fraser and W. Klemperer, J. Chem. Phys. 83 (1985) 6201

[6] J.A. Odutola, T.R. Dyke, B.J. Howard and J.S. Muenter, J. Chem. Phys. 70 (1979) 4884

[7] W. Hagen and A.G.G.M. Thielens, Spectrochimica Acta 38A (1982) 1203

[8] G.C. Pimentel, M.O. Bulanin and M. van Thiel, J. Chem. Phys. 36 (1962) 500
G. Ribbegard, Chem. Phys. 8 (1975) 185

[9] M. Snels, R. Fantoni, M. Zen, S. Stolte and J. Reuss, Chem. Phys. Lett. 124 (1986) 1

[10] M. Snels and R. Fantoni, to be published

[11] J.Geraedts, S. Stolte and J. Reuss, Z. Phys. A304 (1982) 167

[12] K. Shimoda, Y. Ueda and J. Iwahori, Appl. Physics 21 (1980) 181

[13] S.G. Kukolich, Chem. Phys. Lett. 5 (1970) 401

[14] T. Shimizu, F.O. Chimizu, R. Turner and T. Oka, J. Chem. Phys. 55 (1971) 2822

[15] P.A. Kollmann and J.C. Allen, J. Am. Chem. Soc. 93 (1971) 4991
Z. Latajka and S. Scheiner, J. Chem. Phys. 81 (1984) 407

[16] M.J. Frisch, J.A. Pople and J.E. del Bene, J. Phys. Chem. 89 (1985) 3664
J.E. del Bene, private communication

[17] Ian M. Mills, J. Phys. Chem. 88 (1984) 532

[18] A.-M. Sapse, D.C. Jain, Chem. Phys. Lett. 124 (1986) 517

[19] Z. Bacic, U. Buck, H. Meyer and R. Schinke, Chem. Phys. Lett. 125 (1986) 47

IR DISSOCIATION OF DIMERS OF HIGH SYMMETRY MOLECULES: SF_6, SiF_4 AND SiH_4.

M. SNELS AND R. FANTONI*

Fysisch Laboratorium, Katholieke Universiteit
Toernooiveld 6525 ED Nijmegen, The Netherlands

*Permanent adress : ENEA-Dip. TIB, C.R.E., C.P. 65, 00044 Frascati, Roma, Italy

ABSTRACT

IR dissociation of SF_6-, SiF_4- and SiH_4-dimers has been observed by using a bolometer (at 4.2 K) as molecular beam detector. The obtained dissociation spectra in the frequency-range from 880 cm^{-1} to 1100 cm^{-1} are discussed in terms of vibrorotational transitions of the monomer.
A model which assumes freely rotating constituents accounts for most of the observed features.
Typical dimer parameters, such as the bond distance and the relative dimer concentration in the molecular beam have been obtained.

Present work examines the IR-predissociation of dimers constituted by high symmetry molecules. Dimers from several different molecules were predissociated upon interaction with 9 - 11 μm CO_2 laser radiation [1-6]. Whereas low symmetry molecules have shown to give rise either to broad peaks in the dimer spectra (only very recently some structure has been observed in C_2H_4 dimers [1,2]), or to complicated structures as in the cases of NH_3- [3] and CF_3Br- [4] dimers, the dimer spectra of SF_6, SiF_4 and SiH_4 are relatively simple. Clusters containing SF_6 have been studied extensively by using a mass spectrometer [5] or a bolometer [6] as a molecular beam detector. SiF_4-clusters have been studied before [4]; on the dissociation of SiH_4-clusters no data were available, probably because there is hardly an overlap between the emission lines of the CO_2 laser and the absorption spectrum of SiH_4.

The three molecules studied all possess a threefold degenerate mode in the frequency range 880 - 1100 cm^{-1}. A simple model has been proposed [5] to explain the dissociation spectra of SF_6-clusters excited near the frequency of the threefold degenerate ν_3 mode of the monomer. The model, reviewed in the theoretical section, yields a stick spectrum which can account for the positions and the relative intensities of the two peaks in the dimer spectrum of SF_6. Also the isotopic shifts and the relative abundances in the dimer spectrum of SF_6 are properly predicted. Other spectral features can be explained in terms of heavier clusters.

Previous mass-spectrometric measurements on SF_6-clusters [5] provided some information on relative concentrations of different cluster species for various beam conditions. In the present work a bolometer used as a molecular beam detector has a sensitivity which is a factor 100-500 better than that of a mass spectrometer. In addition the spectral information is much more detailed than obtained before [4-6], since we use laser lines of three different gases.

In the next section the experimental apparatus is described and the data processing is discussed. In the third section we will discuss a model which treats the dimers as two freely-rotating sub-units, which interact during excitation through resonant dipole-dipole forces. Subsequently, in the fourth section, the data on the three systems are presented and compared with the calculated dimer spectra according to the proposed model. In the last section we will discuss the concentration of the dimers under the used beam conditions,

the dimer parameters which have been determined and finally the isotopic selectivity of the dimer dissociation

EXPERIMENTAL

The apparatus

The molecular beam apparatus is sketched in fig 1 The beam is produced by the supersonic expansion of a mixture of the studied molecule and He through a 30 μm diameter nozzle into a vacuum chamber which is evacuated by a 1000 l/s oil diffusion pump backed by a 80 m^3/h rotary pump The nozzle temperature can be varied between -50 °C to 150 °C and is stabilized within 0.1 °C

A conical skimmer of 1 1 mm diameter separates the first chamber from the second one which is pumped by a 1000 l/sec oil diffusion pump backed by the same 80 m^3/h rotary pump In this chamber the molecular beam is crossed by the radiation from a CW CO_2 laser The laser with a cavity length of 1 95 m can be operated single-mode with $^{12}CO_2$, $^{13}CO_2$ and N_2O, providing more than 250 laserlines between 880 and 1100 cm^{-1}

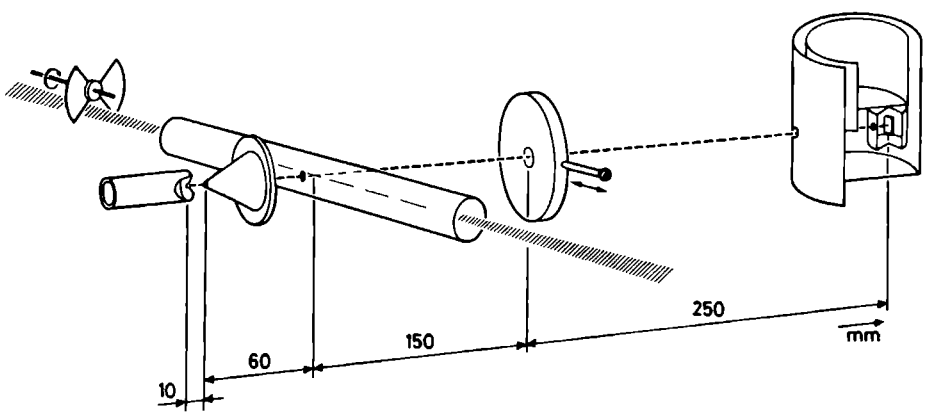

Fig.1 Experimental set-up

The long time power stability is better than 1 % , the frequency stability better than 1 MHz. A piezo-electric translator, mounted on the laser grating, allows a 75 MHz fine tuning of the laser frequency within each laserline. The laser beam is gently focussed to a spot of 0.8 mm diameter on the molecular beam axis.

The third chamber which contains the bolometer is pumped by a 3000 l/sec oil diffusion pump backed by a 12 m^3/h rotary pump. Under typical source conditions , the pressures in the three chambers are $p_1 = 10^{-4} - 10^{-3}$ torr, $p_2 = 10^{-6} - 10^{-5}$ torr and $p_3 = 10^{-7}$ torr. The distance between laserspot and bolometer is 400 mm. As bolometer serves -on a substrate of sapphire (2 mm × 5 mm)- a doped Ge detector of 1 mm x 1 mm (Infrared Laboratories) typically operated at 4.2 K. The N.E.P. at 4.2 K is $4.8 \cdot 10^{-13}$ $WHz^{-1/2}$, the responsivity $5 \cdot 10^4$ V/W and the response time 2.5 ms. During the measurements the response time increases due to so called cryofrost , which is formed by condensation of molecules on the cold detector surface. The bolometer is well shielded from external sources of heat radiation by screens at temperatures of 77 K and 4.2 K and from the laser straylight by several screens between laser and detector.

Gas samples from Matheson (Research Purity) have been diluted by ultra high purity He (99.998%); monomer concentrations between 5% and 1% in He have been used throughout the measurements here reported. The use of SF_6 does not ask for special cautions. The He-mixture containing the highly corrosive SiF_4 gas has been prepared in a specially built monel vacuum line supplied with water filters. The He-mixture containing the highly inflammable SiH_4 gas has been prepared in a carefully pumped reservoir, flushed first by a H_2 flow and subsequently by a SiH_4 flow for several days. Special care has been taken to avoid any presence of oxygen even in the rotary pumps by flowing nitrogen through the ballast valve; metallic tubes have been used for discharge. In spite of the dilution (2% of SiH_4 in He), the pump oil suffered from SiO_2 dust-particle formation, after about 100 working hours.

The measurements

The dissociation spectra were obtained working with a continuous molecular beam and modulating the radiation of the laser. The modulated bolometer signal was amplified by a preamplifier (Infrared Laboratories LN-6C) and fed into a lock-in amplifier. The lock-in signal has been averaged by a microcomputer (Rockwell Aim 65), after subtracting the contribution of the straylight of the

laser, i e the laser-induced signal present even when the molecular beam was switched off The straylight contribution was strongly reduced by directing the laserbeam through a blackened tube with two 5 mm diameter holes to transmit the molecular beam A straightforward correction procedure [6] has been followed in order to account for the linear decrease of the bolometer sensitivity during each run of measurements This decrease of sensitivity was caused by an increase in the response time during the experiment Full spectra obtained at different days were reproduced within 5%, and in most of the cases even within 2%.

The detection of cluster dissociation by a bolometer has some serious drawbacks One of them is the lack of mass-selectivity Furthermore, the heavier a cluster the more efficiently its dissociation is detected (this factor can be easily taken into account provided that the dissociation spectrum of different cluster sizes is known). The third disadvantage is that cryofrost can be a severe problem (heavy cryofrost causes spikes on the bolometer signal which after a short time makes further measurements impossible) and prevents using other than very diluted mixtures. Also for this reason we always worked with mixtures containing less than 5 % of the monomer in He As measured with a 5% mixture of C_2H_4 in He [1] our dynamical range was about 3000, i e we detected an effect 3000 times smaller than our maximum cluster dissociation signal, note that the latter is in turn 1500 times smaller than the total molecular beam signal

Its huge sensitivity is one of the advantages of the bolometer with respect to a mass spectrometer If the dissociation spectrum for different cluster sizes can be resolved, one can measure directly the concentration of each species in the original beam. The mass selectivity of the spectrometric detection suffers in fact of the unknown ionization efficiency and fragmentation mechanism, which up to now prevented us to obtain quantitative information on the beam composition.

In order to obtain the dimer (cluster) concentration in the molecular beam, saturation measurements have been performed. The laser power is varied over a sufficiently broad range by wire meshes inserted into the laser beam, thus without affecting the mode structure (laserfrequency).
The magnitude of the total molecular beam signal E can be measured by modulating the beam. Since the bolometer is essentially an energy detector, one has

$$E = E_{He} + E_{kin} + E_{ads} + E_{vib} + E_{rot} \qquad (1)$$

The main contributions come from the total kinetic energy of the molecules E_{kin} and of the carrier gas atoms , E_{He} Any other contribution of He is negligible The low temperatures achieved by expanding diluted mixtures ensure that E_{vib} and E_{rot} are small, nowadays spectroscopic data on molecules cooled in a beam are available [7], so that those terms can be estimated By far the most uncertain term in (1) is E_{ads}, i e the heat released in the physisorption process of the molecule on the cold surface of the detector, since it is strongly dependent on the molecule and on the surface itself Starting the experiment with a clean detector the adsorption occurs on the sapphire surface, but after a rather short time (less than ten minutes, depending on the specific molecule) a layer of molecules from the beam has been deposited Since there is lack of data on adsorption of molecules on a cold surface covered by the same species (e g SF_6 on a SF_6 surface at a few degrees Kelvin), we approximated E_{ads} with the enthalpy of sublimation of the corresponding molecule

In diluted mixtures saturation of a dimer (cluster) dissociation signal can be easily achieved even with a rather low laser power The ratio of the saturation signal over the total molecular beam intensity gives the concentration of each cluster species with respect to the monomer The main uncertainty in the values obtained is related to the estimate of E_{ads}

Since saturation has shown to occur, we have been particularly careful to measure the spectra shown in the fourth section at sufficiently low power in order to avoid this phenomenon.

Furthermore before discussing the molecular cluster dissociation spectra it has to be mentioned that under the present experimental conditions mixed clusters with He are not expected in any appreciable concentration Most of these complexes are very weakly bound [8] More details on this point, as well as on the detection of monomer absorption which can be overimposed to the cluster dissociation signal, will be given in the discussion of experimental results

In this section a model is proposed to calculate the excitation frequencies for dimers and heavier clusters, assuming a perturbation of the monomer frequency caused by that part of the intermolecular potential which depends on the vibrational coordinates q_i. We consider two spherical top molecules without a permanent dipole moment in a weakly bound system. Each of the constituents can be excited by an IR photon of suitable frequency, to a threefold degenerate mode. (In high-symmetry-molecules - T,T_h, T_d, O, O_h, I, I_h point groups - only three-fold degenerate modes are infrared active [17]). We restrict the treatment to two identical monomers or two different isotopic species of heavy atoms in the same monomer molecule. We assume that the molecules interact through a nearly isotropic potential. The high symmetry of the monomers involved and the corresponding absence of a permanent dipole moment are essential for such an assumption, which is supported by the non complete orientation of solid CH_4 in phase II even at 0 K [10]. In general, an isotropic potential between two molecules 1 and 2 can be written as

$$V(R_{12},q_1,q_2) = V_{\text{repulsion}} + V_{\text{dispersion}} + V_{\text{electrostatic int.}}$$

where R_{12} is the intermolecular distance and q_1 and q_2 are sets of normal coordinates of the two molecules. In the studied systems the repulsive and dispersive terms are mainly responsible for the dimer bond; the electrostatic contribution to the bond is expected to be much smaller since we deal with non-polar species. A Taylor expansion of such a potential gives

$$V(R_{12},q_1,q_2) = V(R_{12}) + \frac{\partial V}{\partial q_1} q_1 + \frac{\partial V}{\partial q_2} q_2 + \frac{1}{2}\frac{\partial^2 V}{\partial q_1^2} q_1^2 + \frac{1}{2}\frac{\partial^2 V}{\partial q_2^2} q_2^2 + \frac{\partial^2 V}{\partial q_1 \partial q_2} q_1 q_2 + \text{higher order terms}$$

Since we consider a single photon excitation of one of the molecules in the cluster along one of its vibrational coordinates q, the first three terms in the Taylor expansion give no perturbation. The quadratic terms (q_1^2 and q_2^2) cause a shift with respect to the monomer frequency and the mixed term ($q_1 q_2$) couples the excitation in one molecule to that in the other(s), in the cluster. If the

variations of the potential - occurring during the vibration - are mainly ruled by the lowest order electrostatic interaction the term $\frac{\partial^2 V}{\partial q_1 \partial q_2} q_1 q_2$ yields simply a resonant dipole-dipole interaction The advantage of this term is that it can be expressed in transition dipole moments, which have been measured in IR absorption of the monomers This resonant dipole-dipole interaction between two atoms which are excited into (almost) degenerate states is fully treated in [9]. The influence of induced dipole moments has not been considered since the polarizability is very small (the ν_3 mode of SF_6 has no Raman activity and the Raman activity of the ν_4 in SiH_4 [11] and of ν_3 in SiF_4 [12] is rather weak)
Confining ourselves to the resonant dipole-dipole interaction, in first order perturbation theory we calculate the energy shifts with respect to the monomer excited levels and obtain the absorption frequencies In order to determine the transition frequencies in a n-molecule cluster we have to diagonalize a 3n×3n matrix. Here, dimers will be treated in detail, the calculations can be extended to larger systems if their equilibrium structure is known [13].

The dipole-dipole interaction operator H_{dd} can be written as

$$H_{dd} = \{\vec{\mu}_1 \cdot \vec{\mu}_2 - 3(\vec{\mu}_1 \cdot \hat{R}_{12})(\vec{\mu}_2 \cdot \hat{R}_{12})\}/(4\pi\varepsilon_o R_{12}^3) \qquad (2)$$

In this expression $\vec{\mu}_1$ and $\vec{\mu}_2$ are the dipole moment operators non-vanishing if sandwiched between ground- and vibrationally excited-states of molecules (1) or (2). The three-fold degeneracy of the involved vibrations enables us to choose an easy reference frame, as shown on the top of fig 2
The 6×6 matrix for the dimer is shown in the same figure The diagonal terms of this matrix correspond to the energy levels of an excited monomer The off-diagonal elements are the perturbations caused by H_{dd} In the chosen frame the wavefunctions of the monomers are combined to account for the in-phase and out-of-phase excitations along a particular axis of the dimer.

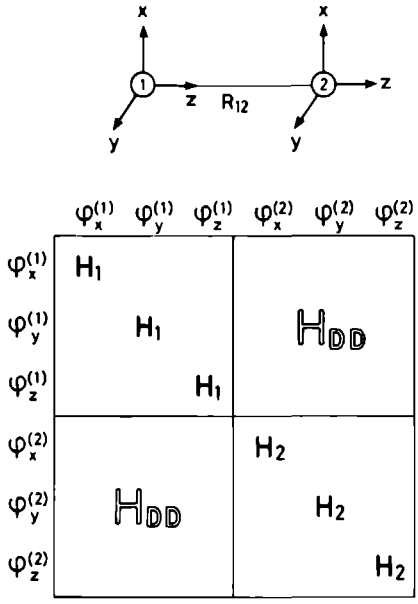

Fig.2 Reference frame and 6 x 6 matrix for dimer.

In the case of two identical constituents (H_1=H_2) these symmetric and anti-symmetry combinations form the eigenfunctions of the vibrationally excited dimer

$$\psi_x^s = \frac{1}{2}(\phi_x^{(1)} + \phi_x^{(2)})$$

$$\psi_x^a = \frac{1}{2}(\phi_x^{(1)} - \phi_x^{(2)})$$

$$\psi_y^s = \frac{1}{2}(\phi_y^{(1)} + \phi_y^{(2)})$$

$$\psi_y^a = \frac{1}{2}(\phi_y^{(1)} - \phi_y^{(2)})$$

$$\psi_z^s = \frac{1}{2}(\phi_z^{(1)} + \phi_z^{(2)})$$

$$\psi_z^a = \frac{1}{2}(\phi_z^{(1)} - \phi_z^{(2)})$$

Here the s and a labelling corresponds to the in-phase and out-of-phase combination of the excitation. Defining

$$\lambda = (\mu_{01})^2 \cdot (4\pi\varepsilon_o R_{12}^3) \qquad (3)$$

we obtain zero off-diagonal elements and the non-vanishing diagonal elements

$$\langle\psi_x^s|H_{dd}|\psi_x^s\rangle = \langle\psi_y^s|H_{dd}|\psi_y^s\rangle = +\lambda$$

$$\langle\psi_x^a|H_{dd}|\psi_x^a\rangle = \langle\psi_y^a|H_{dd}|\psi_y^a\rangle = -\lambda$$

$$\langle\psi_z^s|H_{dd}|\psi_z^s\rangle = -2\lambda$$

$$\langle\psi_z^a|H_{dd}|\psi_z^a\rangle = +2\lambda$$

The eigenvalues correspond to four levels, two of which are two-fold degenerate. The two-fold degenerate levels are the final states for the so-called perpendicular transitions of the dimer [5], the two non-degenerate levels correspond to the parallel dimer transition [5]. The eigenfunctions $\psi_\ell^{s,a}$ (where ℓ = x, y, z) are used to calculate the transition strenghts S according to the expression

$$S = \sum_{\ell} |\langle \psi_{\ell}^{s,a} | \mu_{\ell} | 0 \rangle|^2$$

where $\mu_{\ell} = \mu_{1\ell} + \mu_{2\ell}$ is the sum of the transition dipole moment components of the two monomers along each axis, and $|0\rangle$ stands for the ground state wavefunction. The infrared selection rules require that $\langle \psi_{\ell}^{s,a} | \mu_{\ell} | 0 \rangle \neq 0$; such a restriction is fullfilled only by the ψ_{ℓ}^{s} [5]. Thus, only transitions to the levels displaced by -2λ and $+\lambda$ are allowed, the latter being two-fold degenerate. In this way we obtain a dimer excitation spectrum consisting of two peaks, the shifts with respect to the monomer frequency being respectively -2λ and $+\lambda$, the latter twice as intense as the former.

In the case of two non-identical subunits, for instance of two different isotopes of the same monomer, H_1 and H_2 are different. Diagonalization yields different eigenfunctions and again six eigenvalues corresponding to four different levels (two of which are two-fold degenerate). All the four levels can be reached through infrared excitation, the lowering of symmetry being responsible for weak activity of the two otherwise forbidden transitions [5].

The model discussed up to this point produces a stick spectrum of an n-molecule cluster, hereafter it will be referred as "stick model". The rotational sublevels of the monomers, as well as Coriolis splitting of the degenerate vibrations were neglected. - As a consequence of the assumption of an isotropic potential each constituent is free to rotate in the cluster. Of course only a few rotational levels are really involved , since the considered dimers are produced at low beam temperature.

In the present extended model we consider a dimer consisting of two molecules (1,2) in the vibrational groundstate and with rotational quantum numbers J_1 and J_2 respectively. The groundstate of this dimer is given by $|0,J_1\rangle|0,J_2\rangle$. We assume that only transitions with ΔJ_1, $\Delta J_2 = 0, \pm 1$ can occur. The excited states $|1,J_1'\rangle|0,J_2\rangle$ and $|0,J_1\rangle|1,J_2'\rangle$ (i.e. after vibrorotational excitation of molecule 1 or 2, respectively) yield the diagonal elements H_1 and H_2 in the 6x6 matrix we mentioned before. The energy levels of the excited dimer are calculated by diagonalization of this matrix. Transition frequencies are obtained for all the ground states $|0,J_1\rangle|0,J_2\rangle$ of the dimer weighted by the population of the specific level. This procedure produces a very dense stick spectrum to which we will refer as "free rotor stick spectrum" in order to account at least qualitatively for the free rotation of the molecules in the dimer. All specific

intermolecular potential terms, except the resonant dipole- dipole interaction, pertaining to the $|1,J_1'>|0,J_2>$ and $|0,J_1>|1,J_2'>$ states have been neglected in our approach Details of the known spectroscopic parameters used to simulate the ground and excited levels of each monomer, and about their population distributions will be given in the next section

CLUSTER DISSOCIATION SPECTRA

As already pointed out, the model presented in the previous section has been developped for dimers and clusters of spherical top molecules excited in a three-fold degenerate vibrational mode The SF_6 molecule has an octahedral equilibrium geometry, SiF_4 and SiH_4 both resemble rigid tetrahedrons
The SF_6 monomer has an inversion centre and posseses only two IR active modes of F_{1u} symmetry, respectively ν_3 at 948 0 cm^{-1} and ν_4 at 615 0 cm^{-1} [14], both are threefold degenerate, the ν_3 vibration can be excited by 10 μm laser radiation First order Coriolis interaction between the degenerate components of this mode yields a splitting [15-17] Apart from this interaction, whose magnitude depends on the ζ_3 constant, no significant perturbation from other IR active bands is expected to affect the molecule in its ν_3 vibration
The situation is more complicated in the case of the two tetrahedral molecules [18]. Infrared active modes of F_2 symmetry are ν_3=1031 3969 cm^{-1} and ν_4=388 4 cm^{-1} for SiF_4 [19], and ν_3=2189 08 cm^{-1} and ν_4=913 473 cm^{-1} for SiH_4 [11,20] (the frequencies correspond to excitation of the most abundant ^{28}Si isotope) Interaction with 9 - 11 μm laser radiation involves the three-fold degenerate asymmetric stretching ν_3 for SiF_4 and the three-fold degenerate asymmetric bending ν_4 in the case of SiH_4 As for the ν_3 mode of SF_6, the components of these three-fold degenerate modes are Coriolis coupled, the coupling being ruled by the ζ_3 and ζ_4 constants, respectively Furthermore, a second order Coriolis interaction is possible between levels of F_2 symmetry and levels of E symmetry [17,18] (transitions to the latter are originally IR forbidden). This kind of interaction is especially strong if the interacting levels are rather close
Further details of the spectroscopy for each molecule which are relevant for the present problem will be considered in the discussion of the results

SF_6

In fig. 3 the measured SF_6 cluster dissociation spectrum is compared with the stick spectrum obtained from the original model of [5] and with the dimer spectrum of the $^{32}SF_6$ dimer accounting for the rotational structure of the monomer. On the basis of a previous mass spectrometric investigation of the same clusters, beam conditions were chosen in order to favour the dimers as much as possible. To this purpose 5 atm of a 1% mixture of SF_6 in He was expanded through the 30 μm nozzle at room temperature . The dimer beam was crossed with a 5 W laser beam. The two dimer peaks are evident, as well as two extra features attributed to $^{32}SF_6$-$^{34}SF_6$ isotopically mixed dimers The stick spectrum fits these measurements yielding the parameter $\lambda = 6.8$ cm^{-1} This value is in full agreement with the results of [5] According to the model a trimer contribution is expected to be responsible for some extra intensity on the peak centered at 934 8 cm^{-1} and for the shoulder around 961 cm^{-1}. After fitting λ, experimental intensities and positions for SF_6 dimers are compared in table 1 with the stick model predictions. The natural abundance of ^{34}S (4 21%) has been assumed in the isotope spectrum calculations and leads to a satisfying fit of the experimental data For the present beam conditions a relative trimer/dimer concentration of 5 % has been deduced from the intensity ratio (between the areas) of the trimer peaks with respect to the dimer ones (taking into account the 1 5 higher sensitivity of the bolometer to the heavier species) This shows that a careful choice of the expansion conditions allows a rather pure dimer production. Furthermore present measurements give a strong indication that the SF_6 trimers possess preferentially a geometry of a equilateral triangle, since other geometries do not produce the peaks found around 961 cm^{-1}.

In the discussion of the observed spectrum the possible occurrence of He-SF_6 mixed species has to be considered. The potential well of the He-SF_6 dimer has a depth of ≈43 cm^{-1}, other He-mixed clusters are much weaker bound [8] Previously, a very weak dissociation signal has been indeed observed, on the He mass, upon excitation with the 10P16 (947 74 cm^{-1}),the 10P8 (954.55 cm^{-1}) and the 10P30 (934.90 cm^{-1}) laser lines, due to dissociation of He-SF_6 (10P16) and He-$(SF_6)_2$ complexes (10P8, 10P30), respectively [13]. Since our beam conditions are comparable we do not expect a significant contribution from He-$(SF_6)_n$ complexes to our spectra. Moreover, if dissociation of a He-SF_6 cluster occurs the deflection of the SF_6 fragment with respect to the beam axis will be very small (mass-effect). In fact on our detector (bolometer) we will only observe the loss

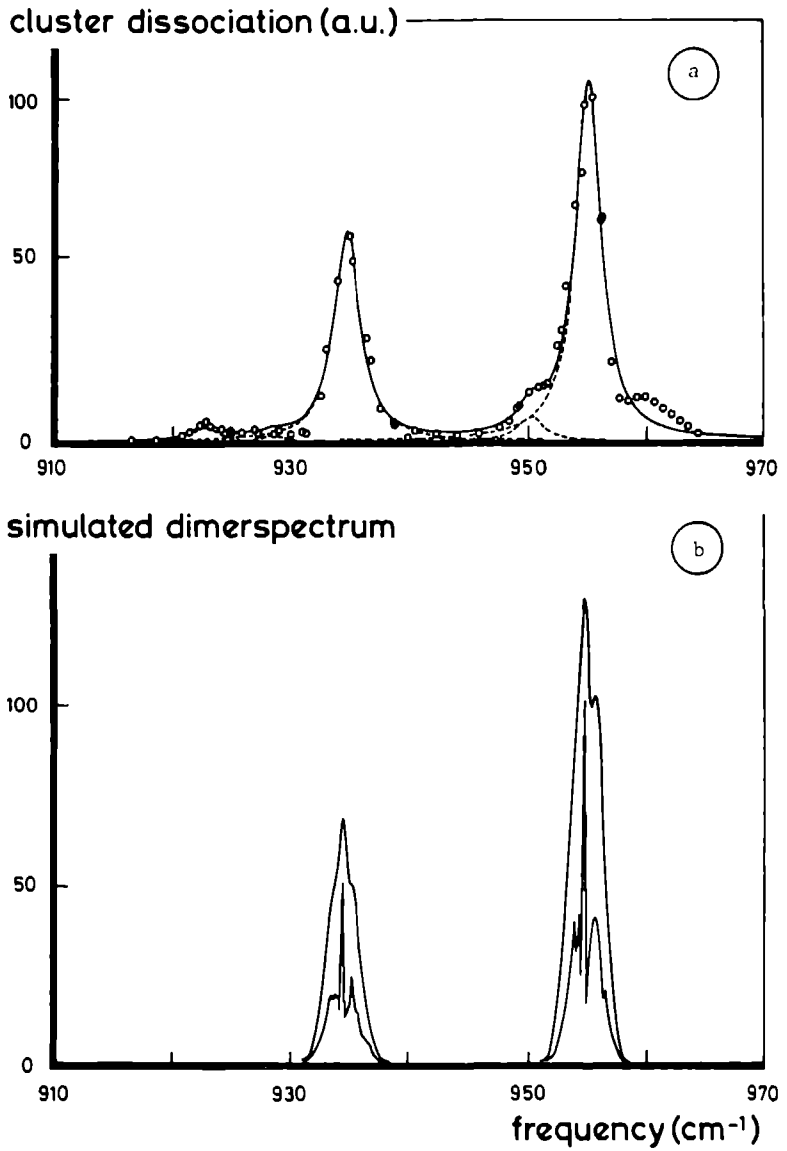

Fig.3 a) Cluster spectrum of 1% SF_6 in He measured at 5 atm and 294 K. The solid line is the best fit. Fitted parameters are given in table 1.

b) Calculated free rotor spectrum with (outer curve) and without (inner curve) the influence of end-over-end rotation.

Table I

SF_6 cluster dissociation

Calculated stickspectrum ($\lambda = 6.8\ cm^{-1}$, $\Delta\nu = 0.0$)				measured spectrum (1% SF_6 in He, 30 μm nozzle, P_0 = 5 bar, T_0 = 294 K)	
peak position (cm^{-1})	cluster species	isotopic abundance (%)	transition intensity (%)	peak position (cm^{-1})	relative intensity* (%)
Dimers					
923.3	$^{32}SF_6$-$^{34}SF_6$	8.0	2.5	922.8	2.3
928.4	$^{32}SF_6$-$^{34}SF_6$	8.0	1.0	928.4	0.9
934.4	$^{32}SF_6$-$^{32}SF_6$	90.3	30.1	934.7	35.2
950.4	$^{32}SF_6$-$^{34}SF_6$	8.0	4.4	950.4	4.1
954.8	$^{32}SF_6$-$^{32}SF_6$	90.3	60.2	955.1	60.2
955.5	$^{32}SF_6$-$^{34}SF_6$	8.0	0.2	955.5	0.2
Trimers					
934.9	$(^{32}SF_6)_3$	85.7	41.3		
957.7	$(^{32}SF_6)_3$	85.7	15.8		
961.6	$(^{32}SF_6)_3$	85.7	28.6		

*Experimental intensities have been normalized on the 954.8 cm^{-1} peak

of an He atom, for which our sensitivity is a factor 80 lower than for two SF_6 molecules in the SF_6 dimer dissociation Note that in case of He-SF_6 dimer dissociation it may even be possible to detect an increase of the bolometer signal, since the SF_6 fragment retains some of the excitation energy Our zero signal at 947 74 cm^{-1} indicates the absence of He-SF_6 dimers in detectable concentrations under present beam conditions

Due to the calorimetric kind of detection adopted in the present experiment, monomer absorption can be observed as well as dimer (cluster) dissociation, the absorption contribution has of course an opposite sign with respect to the dissociation signal (i e excited molecules release extra energy on the bolometer) No SF_6 absorption signal has been detected with laser intensities between 1 - 5 W A piezo-electric scan of the single mode laser emission on the N_2O R10 line performed with much lower power (≈ 25mW) has shown well known absorption lines from low J levels [21]

In fig 3b (inner curves) a calculated SF_6 dimer spectrum is shown for the most abundant ^{32}S isotope in the extended model assuming a rotational temperature of 10 K Molecular parameters for $^{32}SF_6$ monomer in the ground state, B_0=0 0929 cm^{-1}, and in the ν_3 mode at 947 976 cm^{-1} [14], (ζ_3=0 700), B_3=B_0, $B_3\zeta_3$=0 0650 cm^{-1} [15] have been used in the calculation of the vibrorotational energy levels including the Coriolis splitting for the excited states

$$E(\nu_3,+) = \nu_3 + B_3J_1'(J_1'+1) + 2B_3\zeta_3(J_1'+1) + B_0J_2(J_2+1), \quad \text{with } J_1'=J_1-1 \quad (4a)$$

$$E(\nu_3,0) = \nu_3 + B_3J_1'(J_1'+1) + B_0J_2(J_2+1), \quad \text{with } J_1'=J_1 \quad (4b)$$

$$E(\nu_3,-) = \nu_3 + B_3J_1'(J_1'+1) - 2B_3\zeta_3J_1' + B_0J_2(J_2+1), \quad \text{with } J_1'=J_1+1 \quad (4c)$$

In this equation excitation of molecule 1 is assumed. The octahedral field splitting in the vibrationally excited ν_3 levels [16] has been neglected For a temperature of 10 K rotational states up to J=19 have been included in the dimer spectrum calculation Following [17] the population distribution for rotational levels of spherical top molecules, in the limit of high J, has been approximated by the expression

$$P(J) = (2J+1)^2 \cdot \exp[-B_0J(J+1)/kT] \quad (5)$$

Since our calculation yields a high density of lines (10^3 lines/cm^{-1}) only the envelope of the calculated sticks is shown in the figure. The introduction of rotational sublevels including the Coriolis splitting produces an inhomogeneous line width of about 1.6 cm^{-1} on each dimer peak. Simulations for higher temperatures yielded broader spectral features. Previous spectra [5,6] measured with different beam conditions have shown a broadening of the dimer peak as the temperature increases. This trend is properly predicted by the free rotor model. Also dimer-degrees of freedom can be involved in the peak broadening with the increasing of the temperature. Usually van der Waals stretching and bending modes have frequencies of 10 to 50 cm^{-1} and give rise to distinct spectral features [1,2]. Dimer end over end rotation, however, can broaden the dimer peaks.

The broadening induced by dimer end-over-end rotations can estimated, once the dimer rotational constants are known. The rotational constants are calculated (table 6) using the dimer bond distance obtained from λ. The total width of the PQR spectrum is given by [17]

$$\Delta\nu = (8kTB_{eoe}/hc)^{1/2}$$

In our very dense spectrum every stick has been replaced by a gaussian with the calculated width in order to account for the end over end rotation of the dimer. The result obtained in case of T=10 K is also shown in fig. 3b (outer curve); the overall width of each dimer peak is in this case 2.7 cm^{-1}, which is in excellent agreement with the data. The non-lorentzian profile obtained for the dimer peaks reproduces the experimental lineshape rather well; it must be stressed that it is originated by the monomer rotations included in the free rotor model.

Concluding the discussion of the SF_6 cluster dissociation spectrum, we mention that no evidence for combined excitation of van der Waals modes coupled to the ν_3 mode in the dimer has been found in the investigated frequency range from 900 cm^{-1} to 1000 cm^{-1}. Neither has fine structure been observed on the maximum of the dimer peaks with the present piezo-scanning facility (75 MHz full range, 1 MHz resolution).

SiF_4

Fig. 4 displays three spectra of SiF_4 clusters measured at different nozzle temperature (248 K (a), 294 K (b), 323 K (c)) with 1 W laser power. A mixture of 2% SiF_4 in He has been expanded at a pressure of 5 atm. The parameters obtained from a lorentzian fit of those spectra are reported in table 2 As in the case of SF_6 clusters, we observe the two dimer peaks Their intensity ratio is in rather good agreement with the 1:2 prediction of the stick model, but the red one is clearly broader than the blue one. Present results are the first complete spectra of SiF_4 clusters measured in the range 1000 cm^{-1} to 1060 cm^{-1}, since in [4] only the onset of the red peak could be observed by using the $^{12}CO_2$ laser lines. The stick model yields λ= 7.2 cm^{-1} for SiF_4 dimers. Results of dimer and trimer calculations are summarized in table 3.

Table 2

2 % SiF_4 in He , 30 μm nozzle, P_0 = 5 atm.

Nozzle temperature	248 K	294 K	323 K
position peak A	1016.2 cm^{-1}	1015.8 cm^{-1}	1015.5 cm^{-1}
position peak B	1037.8 cm^{-1}	1037.4 cm^{-1}	1037 5 cm^{-1}
FWHM peak A	8.0 cm^{-1}	8.4 cm^{-1}	9.9 cm^{-1}
FWHM peak B	6.5 cm^{-1}	5.9 cm^{-1}	5.5 cm^{-1}
maximum int. A (a.u.)	311	134	45
maximum int. B (a.u.)	439	254	95

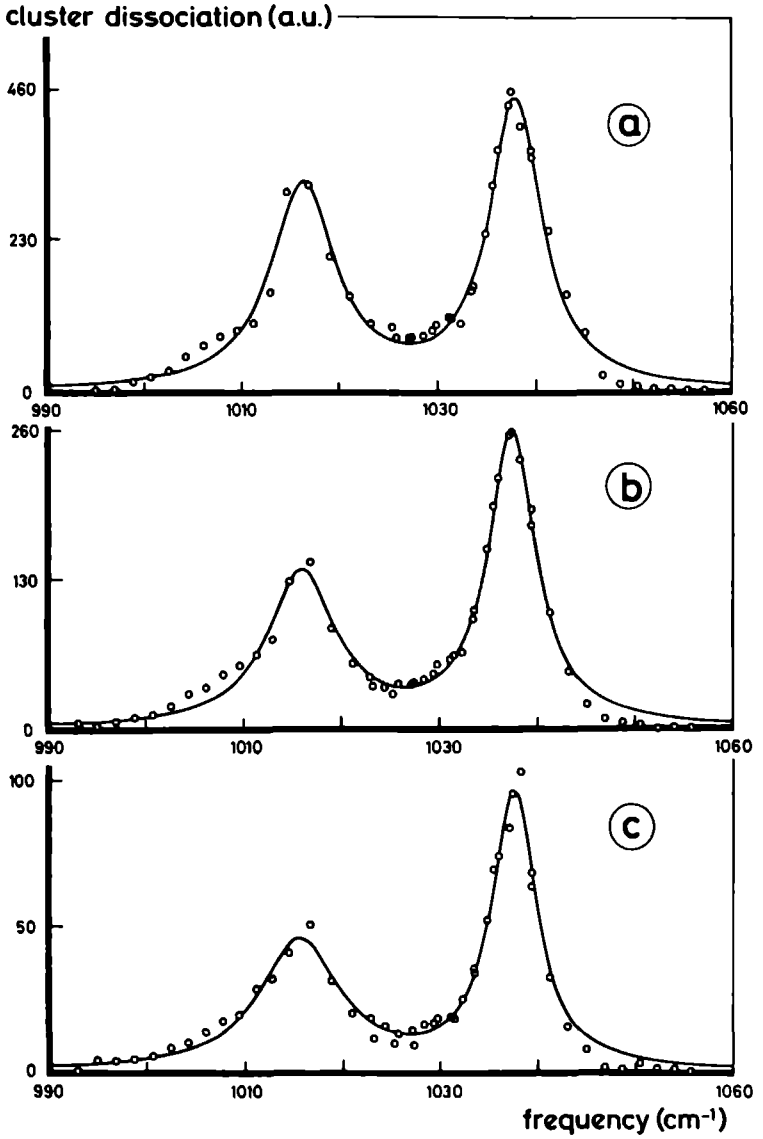

Fig.4 Cluster spectrum of 2% SiF_4 in He measured at 5 atm and nozzle temperatures of 248 K (a), 294 K (b) and 323 K (c). The solid line are best fits. Fitted parameters are given in table 2.

In the coldest spectrum (fig 4a) large trimer contributions are expected under the red shifted dimer peak and on the high frequency side of the blue-shifted one The intensity of the red peak is indeed increased by further cooling the nozzle, but no extra feature appears around 1040 cm^{-1} This fact is rather surprising, even for other than the triangular trimer structure, most intense trimer contributions have been calculated in that frequency region A weak signal attributed to trimers has been observed in [13] under different beam conditions (1500 torr of a 5% SiF_4 mixture in He expanded through a 30 μm nozzle at T=199 K) The absence of observable structure due to SiF_4 trimers in our spectra is strange,the SF_6 spectra show clearly that even a small trimer fraction can be observed Of course the bond distance in the trimer might be different from that in the dimer, which implies that the trimer peak positions have to be calculated using a different value for λ If we take a 15 % larger trimer bond distance, the trimer peaks would be hidden under the dimers Another explanation could be that the trimer peaks are very broad, due to internal motions in the complex In that case they do not give rise to a distinct observable structure

In fig 5 the purest dimer spectrum measured at T_{nozzle}=323 K (a) is compared with the free rotor sticks calculated for $^{28}SiF_4$ dimers at 20 K, (b) inner curve, dimer rotations at the same temperature are accounted for in the outer curve In the stick model the peak positions calculated also for the ^{29}Si and ^{30}Si isotopic species (whose abundance is respectively 4 71% and 3 10%), have been obtained by fitting the parameter λ and allowing also for an additional shift of the spectrum with respect to the monomer frequency A red shift of 1 1 cm^{-1} with respect to ν_3 = 1031 3968 cm^{-1} of [19] yielded the best fit (table 3) The value λ = 7.2 cm^{-1} differs from the preliminary value λ = 6 2 cm^{-1} [4] obtained only from a partial fit The assumption of natural abundance for the Si isotopes leads to a satisfying fit of the experimental data (fig 5a).
The free rotor stick calculation (fig 5b) has been performed assuming a beam temperature of 20 K and including rotational levels up to J=26 The monomer excited levels have been obtained from the scalar energy expressions given in [22] which include distortions up to the fourth order; the tensorial terms have been neglected The analytical expressions for the energies are analogous to (eq 4). Significant spectroscopic parameters are $B_0 \approx B_3$ = 0.13814 cm^{-1} and $B_3\zeta_3$=0 0743 cm^{-1}, (ζ_3=0 534).

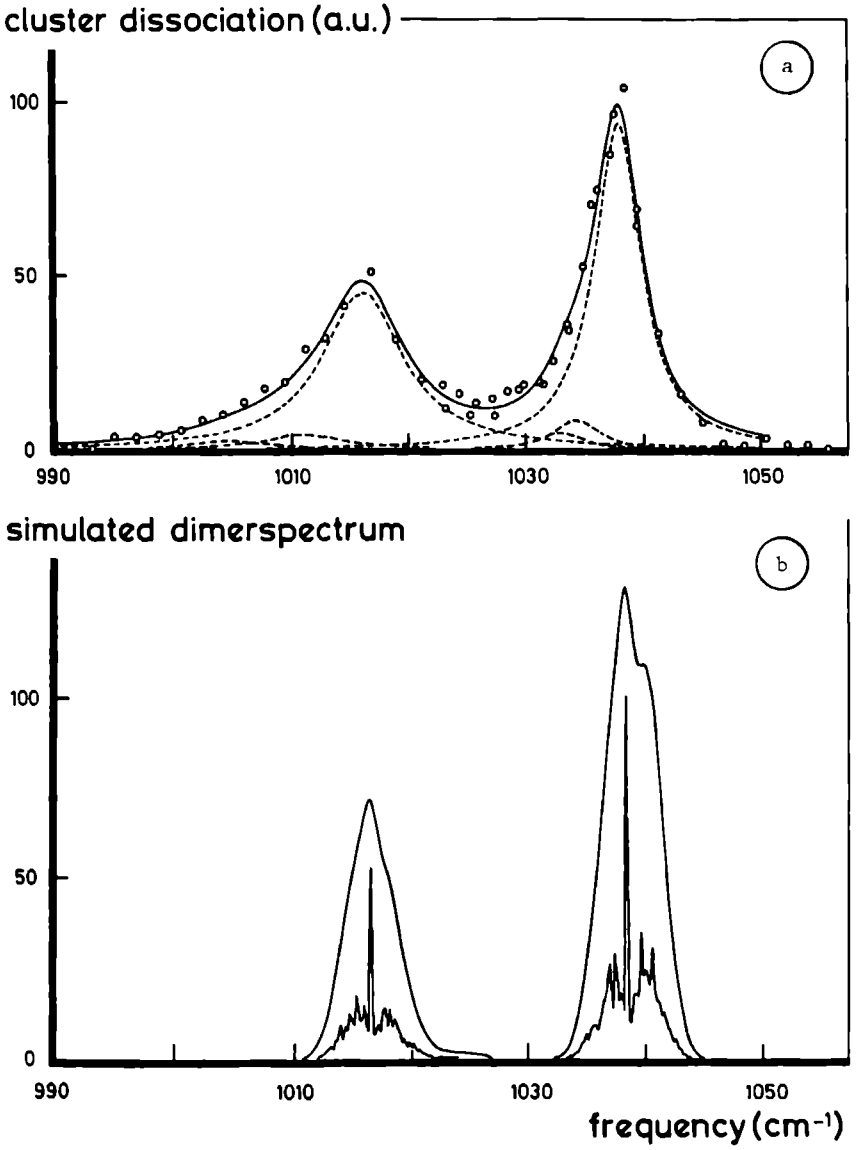

Fig.5 a) Cluster spectrum of 2% SiF_4 in He measured for 5 atm and 323 K The solid line is the best fit. Fitted parameters are given in table 3.

b) Calculated free rotor spectrum with (outer curve) and without (inner curve) the influence of end-over-end rotation.

Table 3

Calculation of dimer and trimer stickspectra for SiF_4 isotopes

(λ = 7.2 cm^{-1}, $\Delta\nu$ = -1.1 cm^{-1})

peak position (cm^{-1})	cluster species	isotopic abundance (%)	transition intensity (%)
Dimers			
1004.8	$^{28}SiF_4$-$^{30}SiF_4$	5.7	1.8
1010.3	$^{28}SiF_4$-$^{30}SiF_4$	5.7	0.7
1010.7	$^{28}SiF_4$-$^{29}SiF_4$	8.7	2.8
1015.9	$^{28}SiF_4$-$^{28}SiF_4$	85.0	28.3
1017.3	$^{28}SiF_4$-$^{29}SiF_4$	8.7	0.4
1032.9	$^{28}SiF_4$-$^{30}SiF_4$	5.7	3.1
1034.3	$^{28}SiF_4$-$^{29}SiF_4$	8.7	5.4
1037.5	$^{28}SiF_4$-$^{28}SiF_4$	85.0	56.7
1038.4	$^{28}SiF_4$-$^{30}SiF_4$	5.7	0.13
1040.9	$^{28}SiF_4$-$^{29}SiF_4$	8.7	0.07
Trimers			
1016.4	$(^{28}SiF_4)_3$	78.4	37.8
1040.6	$(^{28}SiF_4)_3$	78.4	14.4
1044.7	$(^{28}SiF_4)_3$	78.4	26.2

The population of the initial rotational sublevels has been calculated taking into account the nuclear spin statistics g_J ($I_F = 1/2$) in the tetrahedral symmetry [17]

$$P(J) = g_J(2J+1)\cdot\exp[-BJ(J+1)/kT] \qquad (6)$$

It has been verified that for high J g_J in SiF_4 converges to the approximate (2J+1) factor used for SF_6 (eq. 5). The result of the free rotor model calculation yields again two peaks, roughly in the same intensity ratio. The experimental trend of broader peaks for SiF_4 than for SF_6 is well predicted by the present model; the larger rotational constant of SiF_4 is responsible for that.

The end over end rotation of the dimer has been included in the calculation as for SF_6; it produces a further broadening of the dimer spectrum. In fig. 5b (outer curves) it is shown that a width of 4.9 cm^{-1} is obtained at 20 K; the width calculated at 10 K was 3.6 cm^{-1}. The profile of the calculated dimer peaks is rather similar to the measured one (in fig. 5a).

The calculations cannot account for the larger width of the SiF_4 dimer peak centered at -2λ with respect to the one centered at $+\lambda$. Again the knowledge of the monomer spectroscopy can help to understand this phenomenon. In [22] the infrared forbidden combination $\nu_1+\nu_2$ of E symmetry has been observed at 1062.4 cm^{-1}. The (weak) activity of this band has been attributed to Coriolis coupling with ν_3 through the F_2 - E interaction allowed in the T_d point group. Unfortunatly, as pointed out in [19], spectroscopic data available on SiF_4 are not sufficient to calculate the ν_3 / $(\nu_1+\nu_2)$ dyades; however, the result is a repulsion between the interacting levels. The repulsive effect may be responsible for the broadening of the red shifted dimer peak.

As in the case of SF_6 dimers, neither evidence for van der Waals modes coupled to ν_3 ,in the range 1000 - 1060 cm^{-1}, nor rotational fine structure near the maximum of the dimer peaks has been found.

SiH_4

Fig. 6 shows the dissociation spectra of SiH_4 cluster measured with 5 W laser power at three different nozzle temperatures (T=248 K (a), T=294 K (b), T=323 K (c)), for a 5 atm expansion of 2% SiH_4 in He. Again two peaks are present, but their intensity ratio seems reversed with respect to the stick model prediction; even for the highest nozzle temperature this ratio does not approach 1 : 2. The parameters obtained by fitting the measured positions with two lorentzians are listed in table 4. The fit of the dimer stick spectrum yields λ=4.2 cm^{-1} and a red shift of 1.4 cm^{-1} with respect to the value given in [20]. The dimer and trimer stick spectra, also for ^{29}Si and ^{30}Si isotopes, calculated for this λ are listed in table 5.

In Fig. 7 the SiH_4 dimer dissociation spectrum measured at the highest nozzle temperature (a) is compared to the free rotor model, (b), the calculation including also the dimer end over end rotations is shown in the same figure (outer curve). In these calculations only ^{28}Si has been considered.

Table 4

2 % SiH_4 in He , 30 μm nozzle, P_0 = 5 atm.

Nozzle temperature	248 K	294 K	323 K
position peak A	903.7 cm^{-1}	903.8 cm^{-1}	904.1 cm^{-1}
position peak B	916.3 cm^{-1}	916.6 cm^{-1}	916.4 cm^{-1}
FWHM peak A	5.1 cm^{-1}	5.3 cm^{-1}	6.1 cm^{-1}
FWHM peak B	8.3 cm^{-1}	9.3 cm^{-1}	9.6 cm^{-1}
maximum int. A (a.u.)	298	96	48
maximum int. B (a.u.)	174	56	37

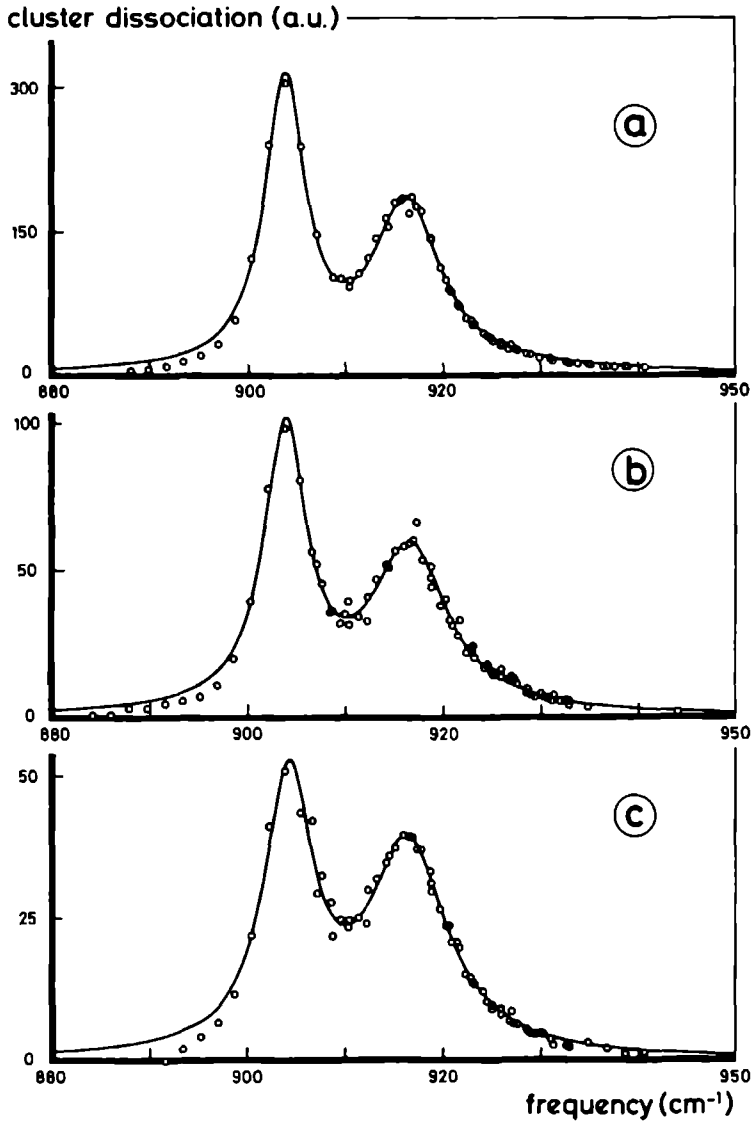

Fig.6 Cluster spectrum of 2% SiH_4 in He measured at 5 atm and nozzle temperatures of 248 K (a), 294 K (b) and 323 K (c). The solid line are best fits. Fitted parameters are given in table 4.

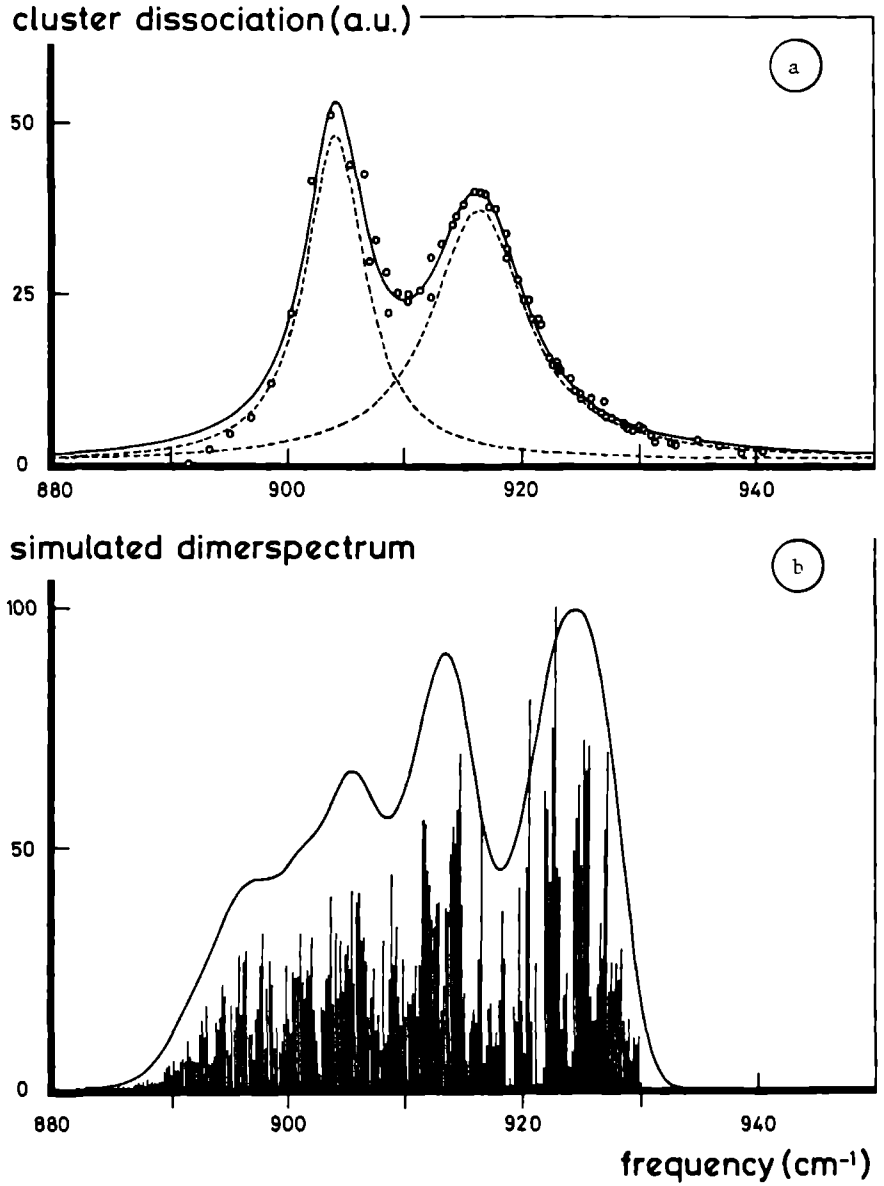

Fig.7 a) Cluster spectrum of 2% SiH_4 in He for 5 atm 323 K
The solid line is the best fit. Fitted parameters are given in table 5.

b) Calculated free rotor spectrum with (curve) and without (sticks) the influence of end-over-end rotation.

Table 5

Calculated dimer and trimer stickspectra for SiH_4 isotopes

(λ = 4.2 cm^{-1}, $\Delta\nu$ = -1.4 cm^{-1})

peak position (cm^{-1})	cluster species	isotopic abundance (%)	transition intensity (%)
Dimers			
902.3	$^{28}SiH_4$-$^{30}SiH_4$	5.7	1.9
903.0	$^{28}SiH_4$-$^{29}SiH_4$	8.7	2.9
903.7	$^{28}SiH_4$-$^{28}SiH_4$	85.0	28.3
906.4	$^{28}SiH_4$-$^{30}SiH_4$	5.7	0.08
907.2	$^{28}SiH_4$-$^{29}SiH_4$	8.7	0.03
915.2	$^{28}SiH_4$-$^{30}SiH_4$	5.7	3.7
915.7	$^{28}SiH_4$-$^{29}SiH_4$	8.7	5.8
916.3	$^{28}SiH_4$-$^{28}SiH_4$	85.0	56.7
919.3	$^{28}SiH_4$-$^{30}SiH_4$	5.7	0.02
919.9	$^{28}SiH_4$-$^{29}SiH_4$	8.7	0.00
Trimers			
904.0	$(^{28}SiH_4)_3$	78.4	37.8
918.1	$(^{28}SiH_4)_3$	78.4	14.4
920.5	$(^{28}SiH_4)_3$	8.4	26.2

The free rotor spectrum has been calculated for $^{28}SiH_4$, with B_0=2 859065 cm^{-1}, ν_4=913 473 cm^{-1}, B_4=2 85720 cm^{-1} and $B_4\zeta_4$=1 4424 cm^{-1} [23], also taking into account the F_2 - E Coriolis interaction of ν_4 with the ν_2 mode at 970 934 cm^{-1}, ($\zeta_{2,4}$=0 582 [11]) Energy levels and transition frequencies for the ν_4 / ν_2 dyades have been taken from [20] (a full list was available), scalar and tensorial parameters up to the fifth order are included in the used Hamiltonian The intensity for each monomer transition up to J=5 [20] has been calculated for T = 20 K This calculation shown in fig 7b accounts for the repulsive effect of the ν_2 levels on the ν_4

In the case of SiH_4 the results of the free rotor model calculation are completely different from those obtained for SF_6 and SiF_4 A very structured spectrum was obtained in the free rotor model which does not reproduce the measured spectrum at all, only a tendency to the observed broadening of the peaks and mixing of the intensity emerged

A gaussian width of 2 86 cm^{-1}, due to dimer rotation, has been attributed to each calculated stick The result is shown in Fig 7b In spite of the similarities between SiH_4 and SiF_4, the present model is not adequate to explain the measured silane dimer spectrum The large amplitude bending ν_2 mode of SiH_4 may inhibit free rotation A more or less locked geometry yields a dimer spectrum consisting of two peaks Internal degrees of freedom of the dimer may be responsible for the observed linewidth

In vain we have tried to detect evidence of dimer dissociation around the ν_2 frequency Coriolis interaction is required to render the ν_2 mode IR-active, this interaction is effective especially for high J levels [20], which are not populated in our expanding beam, this explains the failure of our attempt

Van der Waals modes coupled to ν_4 have not been found in the investigated range 880 - 1000 cm^{-1}, and neither any fine structure on the top of the dimer peaks

We conclude this discussion with some general remarks Differences between $(SiF_4)_2$ and $(SiH_4)_2$ can be attributed to a more locked geometry for the SiH_4 dimer The absence of blue shifted trimer peaks is a striking feature common to both the species At variance with SiF_4 dimers, the SiH_4 dimers exhibit the expected broadening on the dimer peak at $+\lambda$ as the beam temperature is increased

Dimer concentration in the beam

It has been shown before [5,24] that sufficiently high laser power at one laser line can cause the dissociation of all the dimers present in a molecular beam This does not contradict the inhomogeneous broadening of the dimer peaks described by the dressed stick model Since many transitions starting from one dimer ground state level are possible, it is sufficient that there is a coincidence of one of these with a chosen laser line under the line profile Our calculations show that this condition is fullfilled with a life-time broadening of only 0.1 cm^{-1} This agrees with the fact that we do not see any structure in our scans over 75 MHz As discussed in the experimental section, saturation measurements on a dimer (cluster) dissociation peak allow to obtain the relative concentration of that species produced in the beam expansion The dimer dissociation signal can be saturated most easily for the dimer peak at $+\lambda$ A typical saturation behaviour is shown in fig 8; an initial linear increase with the laser power is followed by saturation The observed linear dependence confirms that for the investigated species the dimer dissociation is a single photon process; it yields an upper limit (equal to one laser photon energy) for the binding energy in the complexes.

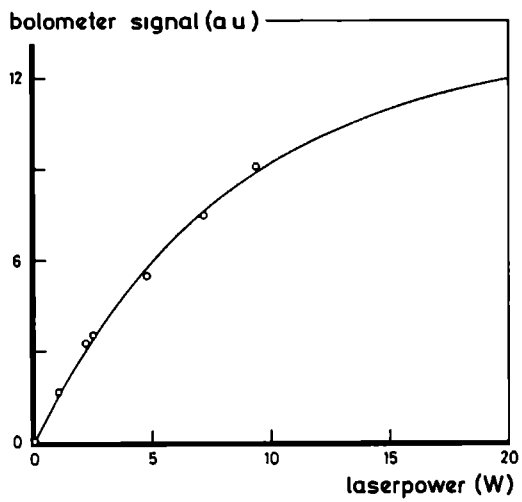

Fig. 8 Saturation behaviour of cluster signal for 2 % SiF_4 in He, 5 atm., 294 K, measured on 9P30

The data shown in fig. 8 have been fitted by a two parameter (S_0, c_1) Lambert-Beer equation

$$S = S_0 \cdot [1-\exp(-c_1 I)] \qquad (7)$$

in which S is the measured dissociation signal intensity and I is the laser power. Since for low laser power the exponential Beer's law is not affected by orientational holeburning effects [25], we can obtain S_0 by extrapolation of the data using eq. (7). For high laser power the value of S corresponds to saturation (S_0) and yields the total dimer signal which has to be compared with the total molecular signal detected on the bolometer ($E - E_{He}$ in eq. (1)). For the investigated systems the sublimation enthalpy of each monomer [26,27] has been used to approximate E_{ads} in Eq(1). Dimer concentrations of 0.33 %, 0.25 % and 0.03 % have been obtained for respectively SF_6, SiF_4 and SiH_4, for beam conditions in which the dimer formation was favoured.

A relative SF_6 trimer/dimer concentration of 5 % has also been obtained from the intensity of the trimer peaks found at 957.7 and 961.6 cm^{-1} with respect to the dimer peak at 954.8 cm^{-1}. This trimer concentration accounts for the extra intensity (a 1.2:2 ratio in stead of the expected 1:2 ratio) measured on the dimer peak at 934.4 cm^{-1}.

Bond distance

As eq. (3) shows the experimental parameter λ is proportional to $\langle R_{12}^{-3} \rangle$, which is the expectation value of R_{12}^{-3}. We estimated how much $(\langle R_{12}^{-3} \rangle)^{-1/3}$ differs from R_0, the equilibrium distance in the dimer, using eigenfunctions of an harmonic oscillator. The difference was smaller than 2 % for SF_6 and SiF_4 and smaller than 5 % for SiH_4. Apparently R_0 is well approximated by $(\langle R_{12}^{-3} \rangle)^{-1/3}$. The values of R_0 obtained in the present measurements are reported in table 6 and compared with the average distance R obtained from density measurements in liquid phase [28]. A systematically shorter bond distance in the case of present gas phase experiments is found.

Another source of information on bond distance are is formed by the measurements of second virial coefficients, polarizability and viscosity. The bond distance derived from these experiments strongly depends on the molecular potential used.

Therefore we prefer to compare our results only with the bond distance more directly deduced from density measurements.

The present values for the dimer bond distance have been used to calculate the dimer rotational constants, also listed in table 6. The highest symmetry dimer configurations have been assumed, a C_4 symmetry about the F-S-F---F-S-F axis for the SF_6 dimer, a C_3 symmetry about the Si-X---Si-X axis for the SiX_4 dimers.

Table 6

Dimerparameters

Molecule	$\lambda(cm^{-1})$	$\mu_{01}(D)$	$R_0(\AA)$	$R(\AA)$	$B_{eoe}(MHz)$
SF_6	6.8	0.387	4.8	5.8[28]	257
SiF_4	7.2	0.276	3.75	4.3[28]	528
SiH_4	4.2	0.21	3.74	4.2[28]	2200

Dissociation energy

With the aim to obtain information about the dimer binding energy, the dimer dissociation has been measured as a function of the nozzle temperature. Results for $(SiF_4)_2$ and $(SiH_4)_2$ are shown in fig. 9 and compared to the NH_3 dimer whose dissociation energy is known to be much higher because of the hydrogen bond [3]. The temperature during the collisional part of the expansion affects the dimer concentration by two different processes. It defines the equilibrium constant for the dimer formation-dissociation reaction, and rules the dimer dissociation due to effective collisions with the carrier gas.

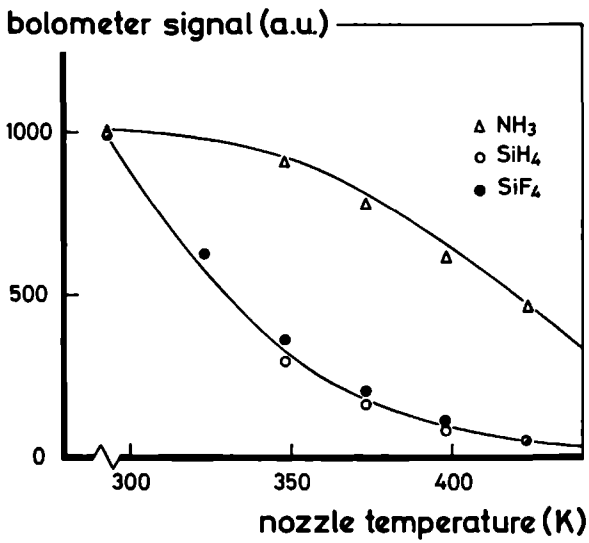

Fig.9 Cluster dissociation versus nozzle temperature for $(NH_3)_2$, $(SiH_4)_2$ and $(SiF_4)_2$. The solid lines are drawn by hand through the experimental points.

Both the processes depend only on the dimer binding energy (heat of formation) in the absence of any barrier In a computer simulation, according to the formulas given in [30], the final dimer concentration has been calculated integrating over the temperature during the expansion and assuming local equilibrium A rather weak dependence on the dimer binding energy has been observed, which is not suitable to interprete the data shown in fig 9.

Isotopic shift

As proposed in [29] infrared photodissociation of dimers (clusters) can be applied to isotope separation With respect to the monomer species, the dimers (clusters) present the advantage to require much less power to be dissociated. Present work has shown that the dimer binding energy is much lower than the energy of one laser photon in the 9 - 11 μm range Single photon dissociation has been obtained on other systems [3] for which a stronger bond was assumed
As shown in table 1 and 3, large isotopic shifts occur also in the dimer if the monomer vibration involves the motion of the isotopic substituent This is the case for ν_3 in SF_6 and in SiF_4; excitation of the ν_4 mode in SiH_4 dimer is less suitable for isotopic separation (see table 5). In fact this mode corresponds with the H - Si - H bending and thus it possesses a small isotopic shift [20].
Furthermore, present experiments have shown that the dimer concentration in the beam is usually a few tenths of a percent only, under beam conditions where the concentration of heavier clusters is minimal. This fact has to be taken into account in evaluating the duty cycle of a laser induced isotope separation which is based on a dimer dissociation scheme

Authors gratefully acknowledge the specialist help of Dr M. Zen and C. Liedenbaum in preparing the bolometer. R. Sanders is thanked for his enthousiastic cooperation during the measurements.
We appreciate very much the encouraging discussions with Prof. J. Reuss and Dr. S. Stolte.
Discussions with Prof. A. van de Avoird and Dr. G. Brocks about the theoretical model were very enlightening. Thanks are due to Drs. G. and C.I. Pierre for sending us their complete results on the ν_4 / ν_2 dyades in SiH_4.
We thank Dr. H. Bluyssen and A. van Etteger who designed our CO_2 laser, and Dr. H. de Moor for helping in the handling of SiH_4. The technical assistance of C. Sikkens and F. van Rijn is also appreciated.

One of us (R.F.) thanks Z.W.O. (Netherlands Organisation for the Advancement of Pure Research) for a fellowship.

REFERENCES

[1] M. Snels, R. Fantoni, M. Zen, S. Stolte, and J. Reuss, Chem. Phys. Lett. 124 (1986) 1

[2] F.Huisken, H. Meyer, C. Launstein, M. Sroza and U. Buck, J. Chem. Phys. 84 (1986) 1042

[3] G.T. Fraser, D.D. Nelson jr., A. Charo and W. Klemperer, J. Chem. Phys. 82 (1985) 2535
M. Snels et al., to be published.

[4] J. Geraedts, M. Snels, S. Stolte and J. Reuss, Chem. Phys. Lett. 106 (1984) 377

[5] J. Geraedts, S. Stolte and J. Reuss, Z. Phys. A 304 (1982) 167

[6] T.E. Gough, D.G. Knight, P.A. Rowntree and G. Scoles, to be published.

[7] G. Luijks, J. Timmerman, S. Stolte, J. Reuss, Chem. Phys. 77 (1983) 169

[8] J.T. Slankas, M. Keil and A. Kuppermann, J. Chem Phys. 70 (1979) 1482
R.T. Pack, E. Piper, G.A. Pfeffer and J.P. Toennies, J. Chem. Phys. 80 (1984) 4940

[9] H. Margenau and N.R. Kestner, "Theory of Intermolecular Forces", Pergamon Press, Oxford 1971 (2nd edition).
J.Hirschfelder, C. Curtiss and R. Bird in "Molecular Theory of Gases and Liquids", J. Wiley and sons Inc., 1964.

[10] M. Sprik, M.L. Klein, J. Chem. Phys. 80 (1984) 988

[11] H.W. Kattenberg and A. Oskam, J. Mol. Spectr. 49 (1974) 52

[12] R.J.H. Clark and D.M. Rippon, J. Mol. Spectr. 44 (1972)479

[13] J. Geraedts PhD. Thesis, Katholic University of Nijmegen 1983
J. Geraedts, M. Waayer, S. Stolte and J. Reuss, Faraday Discuss. Chem. Soc. 73 (1982) 375

[14] Ch.J. Bordé, M. Ouhayoun, A. Van Leberghe, C. Salomon, S. Avrillier, C. D. Cantrell and J. Bordé, in "Laser Spectroscopy", H. Walther and K.W. Rothe Eds., p.142 (Springer Verlag, New York 1979).

[15] P.L. Houston and J.I. Steinfeld, J. Mol. Spectr. 54 (1975) 335

[16] H.W. Galbraith, C.W. Patterson, B.J. Krohn and J. Harter, J. Mol. Spectr., 73 (1978) 475

[17] G. Hertzberg, "IR and Raman Spectra of Polyatomic Molecules", van Nostrand and Co, Princeton N.J. 1959.

[18] G. Wilkinson and M.K. Wilson, J. Chem. Phys. 44 (1966) 3867

[19] R.S Mc Dowell, M.J. Reisfeld, C.W. Patterson, B.J. Krohn, M.C. Vasquez, G.A. Laguna, J. Chem. Phys. 77 (1982) 4337

[20] C.I. Pierre, G. Pierre, G. Guelachvili, A. Valentin and. L. Henry (to be published).
G. Pierre, A. Valentin and L. Henry, Can. J. Phys. (in press)

[21] S Avrillier, J.M. Raimond, Ch.J. Bordé, D. Bassi and G. Scoles, Opt. Commun. 39 (1981) 311

[22] C.W. Patterson, R.S. Mc Dowell, N.G. Nereson, B.J. Krohn, J.S. Wells and F.R. Petersen, J. Mol. Spectr. 91 (1982) 416

[23] D.L. Gray, A.G. Robiette and J.W.C. Johns, Mol. Phys. 34 (1977) 447

[24] M.A. Hoffbauer, K. Liu, C.F. Giese and W.R. Gentry , J. Chem. Phys. 78 (1983) 5567

[25] M. Snels, J.Geraedts, S. Stolte and J. Reuss, Chem. Phys. 94 (1985) 1

[26] American Institute of Physics Handbook, McGraw Hill, 1957, New York.

[27] Landolt-Börnstein, "II band Teil 4", Springer Verlag", 1961, Berlin.

[28] W.M. Sears and J.A. Morrison, J. Chem. Phys. 62 (1975) 2736
E.R.Bernstein and G.R. Meredith, J. Chem. Phys. 67 (1977) 4132
J. Michel, M. Drifford and P. Rigny, J. Chim. Phys. 67 (1970) 31

[29] T.A. Milne, A.E. Vandegrift and F.T. Greene, J. Chem. Phys. 52 (1970) 1552

[30] J.-M. Zellweger, J.-M. Philippoz, P. Melinon, R. Monot and H. van den Bergh, Phys. Rev. Lett. 52 (1984) 522

Chemical Physics 94 (1985) 1–6
North Holland Amsterdam

ORIENTATIONAL HOLE BURNING FOR DIMERS IN THE LIMIT OF LARGE ROTATIONAL QUANTUM NUMBERS [1]

M SNELS, J GERARDTS, S STOLTE and J REUSS

Fysisch Laboratorium, Katholieke Universiteit Nijmegen Toernooiveld 6525 ED Nijmegen The Netherlands

Received 17 August 1984

Dimers can often be treated as prolate symmetric tops with their symmetry axis along the dimer axis In that case thermal excitation results in $J \; M_J \gg K$ if the moment of inertia around the dimer axis can be assumed much larger than the moment of inertia along an axis perpendicular to it Expressions are derived which describe the near saturation behaviour of perpendicular and parallel excitations for $J \; M_J \gg K$ simple analytical expressions are obtained

1 Introduction

In dimer spectroscopy, pulsed and cw lasers are used to predissociate the complexes [1 11] The power available often drives the observed transitions into saturation, with consequent broadening of spectral features and dimer-fractions of a few percent remaining undissociated

Under such circumstances it is not permissible to take into account all possible directions of the dimer axis by introducing a factor 1/3 in front of the squared transition dipole moment, as is common practice in linear spectroscopy There may be "die-hards" amongst the dimers, with orientations such that the polarized laser field is not able to induce transitions An example is given by the parallel transition peak for $(SF_6)_2$ (at 934 9 cm^{-1}, see refs [7–9]) where the induced vibrations along the dimer axis are perpendicular to the laser E-field, if $J = M_J \gg K$, 1 The quantum numbers J and M_J describe the end-over-end rotational angular momentum of the dimer and its projection onto the direction of the laser E-field, the quantum number K stands for the projection onto the dimer axis [12] The dimer axis rotates in a plane perpendicular to the direction of the laser E-field such that $\mu \; E = 0$ and no transitions take place

[1] Work supported by Stichting voor Fundamenteel Onderzoek der Materie (FOM)

On the contrary, orientations with $J \gg M_J$, K, 1 show transitions leading to predissociation and disappear from the collection of dimers This effect is indicated in the title of this paper as orientational hole burning

Treating the case of photodissociation of a diatomic molecule by an electronic transition, Ling and Wilson [13] calculated and demonstrated the effect of orientational hole burning on the photon fragment angular distribution Recently, de Vries et al [14] applied these effects to study the influence of molecular alignment on chemical reaction probability In a numerical analysis Altkorn and Zare [15] showed that by orientational hole burning, saturation strongly influences the polarization of the laser-induced fluorescence (LIF), it has to be taken into account when the M_J-state distribution is to be extracted from LIF measurements

We address ourselves to the IR vibrational excitation of molecular dimers possessing rotational wavefunctions of the prolate symmetric-top type, thus extending the treatment of ref [13] From the limit for large quantum numbers (section 3) simple analytical expressions are obtained, yielding the effect of orientational hole burning on the dissociation probability and lineshape (section 4) Implications for practical cases (i e $(SF_6)_2$ and $(C_2H_4)_2$) are briefly considered In section 5 we will complete this paper stating our conclusions

2 Derivation of the dimer transition matrix elements

The transition strength is governed by the squared matrix element $\mu^2_{fi,z}$, where the subscript z designates the z-component, taken along the direction of the laser E-field

In a molecular fixed frame (ζ-axis along dimer axis) the cartesian components of a vector μ are given by (μ_ξ, μ_η, μ_ζ) The z-component yields

$$\mu_z = \mu_\xi \sin\beta\cos\gamma + \mu_\eta \sin\beta\sin\gamma + \mu_\zeta\cos\beta \quad (1)$$

Here, α, β and γ stand for the Euler angles which transform the space-fixed coordinate system into the molecular fixed one [12]

The initial state (of a symmetrical-top-like molecular complex) is characterized by a rotational wavefunction $|\mathrm{rot}\rangle = (-)^{-M_J+K}[(2J+1)/8\pi^2]^{1/2}D^J_{M,K}(\alpha,\beta,\gamma)$, and a vibrational wavefunction $|\mathrm{vib}\rangle$

Because of the usually low temperature of nozzle beams containing an appreciable fraction of dimers, we assume the dimers to be in their ground vibrational state, $|\mathrm{vib}\rangle = |0\rangle$ The final state is characterized by $|\mathrm{vib}'\rangle$ and $|\mathrm{rot}'\rangle = (-)^{-M_J+K} \times[(2J'+1)/8\pi^2]^{1/2}D^J_{M,K}(\alpha,\beta,\gamma)$ The transition dipole component interacting with an E-field along the z-axis in the laboratory frame is given by

$$\mu_{01,z} = \langle \mathrm{vib}'|\langle \mathrm{rot}'|\mu_\xi \sin\beta\cos\gamma + \mu_\eta\sin\beta\sin\gamma + \mu_\zeta\cos\beta|\mathrm{rot}\rangle|\mathrm{vib}\rangle \quad (2)$$

The excited wavefunction $|\mathrm{vib}'\rangle$ is characterized by the direction of its transition dipole moment with respect to the dimer frame

In mixed dimers where only one of the molecular constituents actually vibrates, $|\mathrm{vib}'\rangle$ can be described by $|\xi\rangle$, $|\eta\rangle$ or $|\zeta\rangle$ The excited vibrational states $|\xi\rangle$, $|\eta\rangle$ and $|\zeta\rangle$ have their transition dipole moments along the ξ-, η- or ζ-axis respectively Linear combinations are admissible

For homo-molecular dimers $|\xi_1\rangle$ for instance means that constituent 1 of the dimer is vibrationally excited with a vibration along the ξ-axis

In case of $(SF_6)_2$ and ν_3-mode excitation the degeneracy among the states $|\xi_i\rangle$, $|\eta_i\rangle$ and $|\zeta_i\rangle$ is partially lifted, due to the resonant dipole–dipole interaction [7] Its "IR active states" (those accessible from the ground state by absorption of an IR photon) are

$$|\mathrm{vib}'\rangle = \left[|\zeta_1\rangle + |\zeta_2\rangle\right]/2^{1/2}, \quad (3a)$$

$$|\mathrm{vib}'\rangle = \left[\left(|\xi_1\rangle + |\xi_2\rangle\right) \pm i\left(|\eta_1\rangle + |\eta_2\rangle\right)\right]/2 \quad (3b)$$

The general case, see eq (2), contains products of three D-functions integrated over α, β and γ A parallel transition yields

$$\mu_{01,z}(\parallel) = \delta_{M_J M_J}\delta_{K K} \times[(2J'+1)(2J+1)]^{1/2}(-)^{-M_J+K} \times\mu_{01}S_\parallel \begin{pmatrix} J' & 1 & J \\ -M_J & 0 & M_J \end{pmatrix} \times \begin{pmatrix} J' & 1 & J \\ -K & 0 & K \end{pmatrix}, \quad (4)$$

with $S_\parallel \equiv \langle \mathrm{vib}'|\mu_\zeta|\mathrm{vib}\rangle/\mu_{01}$ A perpendicular transition yields

$$\mu_{01,z}(\perp) = \delta_{M_J M_J}\delta_{K+1 K} \times[(2J'+1)(2J+1)]^{1/2}(-)^{-M_J+K} \times\tfrac{1}{2}\mu_{01}S^+ \begin{pmatrix} J' & 1 & J \\ -M_J & 0 & M_J \end{pmatrix} \times \begin{pmatrix} J' & 1 & J \\ -(K\pm1) & \pm1 & K \end{pmatrix}, \quad (5)$$

with

$$S^\pm = \langle \mathrm{vib}'|\mp\mu_\xi + i\mu_\eta|\mathrm{vib}\rangle/\mu_{01}$$

Here, μ_{01} stands for the transition dipole moment of the monomer and the coefficients $S_\parallel$, $S^\pm$ describe the relative strength of a specific type of dimer transition Eqs (4) and (5) show that transitions with $J' = J$, $J \pm 1$ are possible

3. The J, $M_J \gg K$, 1 approximation for the transition probability

The transition probability is proportional to $|\mu_{fi,z}(\parallel \text{ or } \perp)|^2$, for a transition from $|JM_JK\rangle|0\rangle$ to a definite final state We consider the sum over all final states leading to the same vibrational

transition frequency, i e $K' = K$, $J' = J$, $J \pm 1$ for the parallel transition and $K' = K \pm 1$, $J' = J$, $J \pm 1$ for the perpendicular transitions The two different sums are indicated by $\Sigma_{\parallel}$ and $\Sigma_{\perp}$

$$\Sigma_{\parallel}\mu^2_{fi} = \Sigma_{\parallel}(2J+1)(2J'+1)\mu^2_{01\,\parallel} \times \begin{pmatrix} J' & 1 & J \\ -M_J & 0 & M_J \end{pmatrix}^2 \begin{pmatrix} J' & 1 & J \\ -K & 0 & K \end{pmatrix}^2,$$

with

$$\mu^2_{01\,\parallel} = |\langle \mathrm{vib}'|\mu_\xi|\mathrm{vib}\rangle|^2, \tag{6a}$$

$$\Sigma_{\perp}\mu^2_{fi} = \Sigma_{\perp}\tfrac{1}{2}(2J+1)(2J'+1)\mu^2_{01\,\perp} \times \begin{pmatrix} J' & 1 & J \\ -M_J & 0 & M_J \end{pmatrix}^2 \times \begin{pmatrix} J' & 1 & J \\ -K' & K'-K & K \end{pmatrix}^2,$$

with

$$\mu^2_{01\,\perp} = |\langle \mathrm{vib}'|\mu_\xi|\mathrm{vib}\rangle|^2 + |\langle \mathrm{vib}'|\mu_\eta|\mathrm{vib}\rangle|^2 \tag{6b}$$

In the following we assume $J \gg 1$

For the parallel transition one has

$$\Sigma_{\parallel}\mu^2_{fi\ z} = \mu^2_{01\,\parallel}\left[(M_J^2K^2)/J^4 + (J^2 - M_J^2)(J^2 - K^2)/2J^4\right] \tag{7}$$

The first term within the brackets originates from the $J' = J$ transitions We assume $K \ll J$ and put $M_J^2/J^2 \equiv \cos^2\theta$ Then

$$\Sigma_{\parallel}\mu^2_{if\ z} = \mu^2_{01\,\parallel}\left[(K^2/J^2)\cos^2\theta + \tfrac{1}{2} - \tfrac{1}{2}\cos^2\theta\right] = \tfrac{1}{2}\mu^2_{01\,\parallel}(1 - \cos^2\theta) + \tag{8}$$

If one takes the usual orientational average $[1/(2J+1)\Sigma_{M_J}]$, a procedure which is equivalent with putting $\overline{\cos^2\theta} = 1/3$, one finds

$$\Sigma_{\parallel}\mu^2_{if\ z} = \tfrac{1}{3}\mu^2_{01\,\parallel}, \tag{9}$$

For perpendicular transitions we proceed similarly and obtain

$$\Sigma_{\perp}\mu^2_{if\ z} = \mu^2_{01\,\perp}\left[\tfrac{1}{2}\cos^2\theta + \tfrac{1}{4}(1 - \cos^2\theta)\right] \tag{10}$$

Here, the first term stems from $J' = J$ transitions, the second from $J' = J \pm 1$ transitions Thus

$$\Sigma_{\perp}\mu^2_{if\ z} = \tfrac{1}{4}\mu^2_{01\,\perp}(1 + \cos^2\theta) \tag{11}$$

and, with the usual average $[1/(2J+1)\Sigma_{M_J}]$,

$$\Sigma_{\perp}\mu^2_{if\ -} = \tfrac{1}{3}\mu^2_{01\,\perp} \tag{12}$$

4. Calculation of beam attenuation and the influence of orientational hole burning

If the interaction time laser–dimer is t and the transition rate r_i, one finds for the probability of predissociation [5,8]

$$r_i t = f_i(\theta)2\pi(F/c)\left(\mu^2_{01}/h^2\varepsilon_0\right) \times \left\{ g_i S_i(\Gamma_i/2)/\left[(\nu - \nu_i)^2 + (\Gamma_i/2)^2\right]\right\}, \tag{13}$$

with [eqs (8) and (9)]

$$f_i(\theta) = \tfrac{1}{2}(1 - \cos^2\theta), \quad \parallel\text{-transition} \tag{14}$$

and

$$f_i(\theta) = \tfrac{1}{4}(1 + \cos^2\theta), \quad \perp\text{-transition} \tag{15}$$

Both f_i expressions yield 1/3 as average over all M_J/J values In eq (13), $h\nu_i$ describes the energy of the ith state and Γ_i its width, g_i stands for the degeneracy of state i and S_i for its relative transition strength, the non-degenerate ground state is given zero-energy The effect of power broadening has been neglected in eq (13) assuming Γ_i (which is typically $\geqslant 1\ \mathrm{cm}^{-1}$), much larger than the Rabi frequency $\mu_{01}E_{\mathrm{laser}}/h$ The laser interaction (laser photon energy $h\nu$) is characterized by the fluence F

In case of the (SF_6)-dimer, the $\parallel$-transition has $S_i = 2$ and $g_i = 1$, the perpendicular one $S_i = 2$ and $g_i = 2$, see refs [8,9]

For molecular beam dimers possessing a single orientation $M_J/J = \cos\theta$ of their angular momentum vector, J, the attenuation due to predissociation is given by

$$A_i(\theta) = 1 - \exp(-r_i t) \tag{16}$$

Averaging over all orientations leads to [9]

$$\overline{A}_i = (1/4\pi)\int\int \mathrm{d}\phi\ \mathrm{d}\cos\theta\, A_i(\theta) = 1 - (1/H_i)\exp(-H_i^2)\int_0^{H_i}\mathrm{d}H\exp(H^2) = 1 - (1/H_i)\mathrm{Daw}(H_i), \tag{17}$$

with $H = H_t \cos\theta$ and $H_t = (3\bar{r}_t t/2)^{1/2}$ for parallel transitions, and

$$\bar{A}_t = 1 - (1/H_t)\exp(-H_t^2)\int_0^H \exp(-H^2)\,\mathrm{d}H$$

$$= 1 - \left(\tfrac{1}{2}\pi^{1/2}/H_t\right)\exp(-H_t^2)\,\mathrm{Erf}(H_t), \qquad (18)$$

with $H = H_t \cos\theta$ and $H_t = (3r_t t/4)^{1/2}$ for perpendicular transitions Here $r_t t$ is defined as the conventional orientational averaged probability on predissociation obtained from eq (13) after putting $f_t(\theta) = 1/3$ In the following we will use $r_t t$ as a saturation parameter The Dawson function, $\mathrm{Daw}(x)$, and the error function, $\mathrm{Erf}(x)$, are tabulated and are also available as standard functions in Fortran

The remaining beam fraction is given by $\bar{R}_t = 1 - \bar{A}_t$, this quantity shows very strong influence of the type of transition considered For strong fluences and ||-transitions eq (16) yields [9]

$$\bar{R}_t(\|) = 1/3r_t t + \qquad (19)$$

Instead of this slow diminuition for increasing values of $\bar{r}_t t$ one finds for strong fluences and perpendicular transitions [9]

$$\bar{R}_t(\perp) = \pi^{1/2}\exp(-3\bar{r}_t t/4)/2(3\bar{r}_t t/4)^{1/2} + \qquad (20)$$

In order to calculate the remaining beam fraction $\bar{R}_t$ for an actual beam of dimers radiated by an IR laser, one has to keep in mind that apart from the distribution over M_J-states, there is also a distribution over internal (i e J) states, each having its individual ν_t-value Since this distribution over ν_t is often quite narrow (low internal temperature of supersonic beam) compared with a typical $\Gamma_t \geqslant 1\ \mathrm{cm}^{-1}$, this extra averaging over ν_t will be neglected For dissociation of dimers by laser photons [3,16] a fluence dependent quantity can be defined which approaches the true cross section in the limit of $r_t t \ll 1$

$$\sigma_{\mathrm{app}} \equiv -(h\nu/F)\ln(\bar{R}_t) \qquad (21)$$

σ_{app} is maximal for $\nu = \nu_t$ and has a spectral profile with a width (fwhm) defined to be equal to Γ if orientational hole burning is neglected, putting $f_t(\theta) = 1/3$ eq (21) simplifies to the expression of the true cross section for dissociation of dimers by photons (for all fluences)

$$\sigma_t = \bar{r}_t h\nu/F \qquad (22)$$

According to eq (13), σ_t has a lorentzian spectral profile with a width Γ_t

$$\sigma_t = (2\pi/3c)\left[(h\nu)\mu_{01}^2/h^2\varepsilon_0\right] \times \left\{(g_t S_t \Gamma_t/2)/\left[(\nu-\nu_t)^2 + (\Gamma_t/2)^2\right]\right\} \qquad (23)$$

To investigate the effect of orientational hole burning [eqs (17) and (18)], we have calculated the remaining fraction, $\bar{R}_t$, of dimers for a parallel and perpendicular transition as a function of fluence F The results for $(SF_6)_2$ are displayed in the upper panel (a) of fig 1 To make this plot useful for a general case the ordinate scale has also been expressed in units of the saturation parameter $\bar{r}_t t$ Especially for parallel transitions the deviations from a pure exponential decay become already considerable for $\bar{r}_t t \geqslant 1\,5$ As indicated by dotted curves the behaviour at high fluences follows asymptotically from eqs (19) and (20) Apparently the "die-hards" amongst the dimers, which possess unfavourable orientations for excitation by the linear polarized laser field, cause the remaining beam fraction $\bar{R}_t$ to lag behind with respect to the pure exponential case This of course leads to a smaller value of the quantity σ_{app}, at larger $\bar{r}_t t$ Together with its asymptotic limits $\sigma_{\mathrm{app}}/\sigma_t$ has been plotted in the middle panel (b) of fig 1 as a function of the laser fluence F (i e as a function of $\bar{r}_t t$ at fixed ν)

The linewidth Γ_{app} is related to the frequency dependence of σ_{app}, which is proportional to $-\ln \bar{R}_t$ Neglecting the hole burning effect we find that $-\ln \bar{R}_t = \bar{r}_t t$ and the linewidth Γ_t corresponds to lowering $\bar{r}_t t$ to half its maximum value at $\nu = \nu_t$, eq (13) Considering now the hole-burning effect we can see in panel (a) of fig 1 that we have to decrease $r_t t$ by more than a factor two in order to halve $-\ln \bar{R}_t$ The value of Γ_{app}, thus larger than Γ_t, is obtained from $|\nu - \nu_t|$ chosen such that the proportionality factor $(\Gamma_t/2)/[(\Gamma_t/2)^2 - (\nu-\nu_t)^2]$ in eq (13) lowers σ_{app} to half its maximum value at $\nu = \nu_t$ The dependence of $\Gamma_{\mathrm{app}}/\Gamma_t$ upon F (for $(SF_6)_2$ as a function of F, and

for the general case as a function of $\bar{r}_i t$, at $\nu - \nu_i = 0$) is shown in panel (c) of fig. 1. As can be deduced from inspecting σ_{app}/σ_i in panel (b), the high-fluence behaviour of $\Gamma_{app}/\Gamma_i \to [(r_i t)^{1/2} - 1]^{1/2}$ for a parallel transition [following from eq. (19)] will be reached at $\bar{r}_i t \gtrsim 10$ and falls outside the range of panel (c).

For small transition rates the asymptotic behaviour of Γ_{app}/Γ_i can be found from eqs. (13) and (21)

$$\sigma_{app} = -(h\nu/F)\ln\left[\overline{\exp(-r_i t)}\right], \tag{24}$$

if the exponent and logarithm are expanded up to terms proportional to $(r_i t)^2$

$$\sigma_{app} = (h\nu/F)\left(\bar{r}_i t - \tfrac{1}{2}\overline{r_i^2} t_i^2 + \tfrac{1}{2}\bar{r}_i^2 t^2\right). \tag{25}$$

With $\overline{f_i(\theta)} = 1/3$ and $\overline{f_i^2(\theta)} = 2/15$ (||-case) and 7/60 ($\perp$-case) [see eqs. (14) and (15)] one obtains non-lorentzian profiles

$$\sigma_{app} = (h\nu/F)\bar{r}_i t\left(1 - \tfrac{1}{10}\bar{r}_i t\right), \quad \|\text{-case}, \tag{26a}$$

and

$$\sigma_{app} = (h\nu/F)\bar{r}_i t\left(1 - \tfrac{1}{40}\bar{r}_i t\right), \quad \perp\text{-case}. \tag{26b}$$

Inserting eq. (13) one calculates

$$\Gamma_{app}/\Gamma_i = 1 + \tfrac{1}{20}\bar{r}_i t, \quad \|\text{-case} \tag{27a}$$

and

$$\Gamma_{app}/\Gamma_i = 1 + \tfrac{1}{80}\bar{r}_i t, \quad \perp\text{-case}. \tag{27b}$$

The starting slopes of fig. 1 are in agreement with these asymptotic expressions.

Besides the theoretical example of $(SF_6)_2$ discussed above, for which no experimental data are

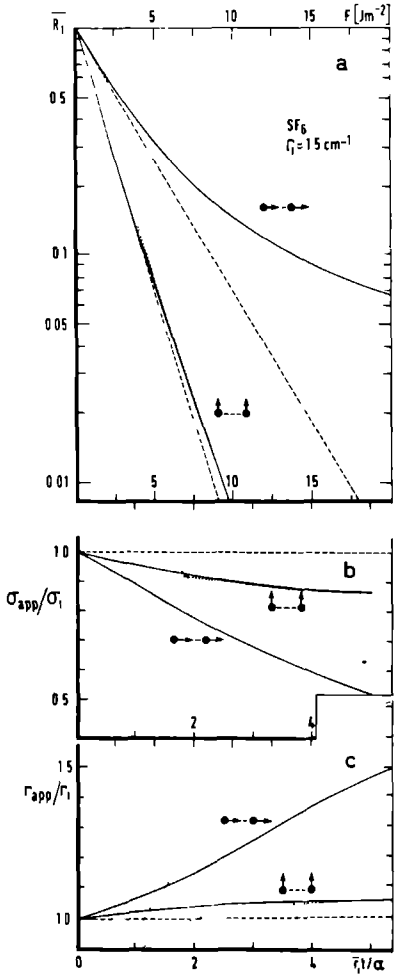

Fig. 1. Influence of orientational hole burning for dimers [e.g. $(SF_6)_2$]. In the upper panel (a) the remaining fraction $\bar{R}_i$ of $(SF_6)_2$ dimers is plotted (———) for a parallel transition (●→ ●→, $\bar{R}_{i,\|}$), and for a perpendicular transition (↑● ●↑, $\bar{R}_{i,\perp}$), as a function of laser fluence F (see upper scale). We use $\Gamma_i = 1.5$ cm^{-1} and $\mu_{01} = 0.387$ D [8,9]. The horizontal scale at the bottom has been chosen in units of $\bar{r}_i t/\alpha$. The scaling factor α has the value 1 and 2 for a parallel and perpendicular transition respectively. For purpose of comparison broken lines (- - - - -) indicate the exponential dependence, which results from a calculation neglecting the orientational hole burning. The dotted curves ( ) indicate the asymptotical behaviour, valid for $\bar{r}_i t \gg 1$, as calculated from eqs. (19) and (20). In panel (b) σ_{app} of eq. (21) R_i is displayed versus F at $\nu = \nu_i$ and versus $\bar{r}_i t/\alpha$. In the bottom panel (c) the reduced spectral width Γ/Γ_i of σ_{app} has been plotted as a function of F. The "general" units of $\bar{r}_i t/\alpha$ relate, for this last case, to the laser frequency at $\nu - \nu_i = 0$. All other notations in panels (b) and (c) as in panel (a).

available at very high fluence *, there is evidence of the observation of orientational hole burning for $(C_2H_4)_2$. Hoffbauer et al. [3], employed pulsed CO_2 lasers with high fluences to measure a spectral width $\Gamma_{app} = 17.5\ cm^{-1}$ of σ_{app}, in contrast to the low fluence value $\Gamma_{app} = 12.1\ cm^{-1}$, obtained by Cassasa et al. [16] and confirmed by Geraedts [17]. This discrepancy has been discussed, in the light of hole-burning effects by Janda [18] and Cassasa [19], Hoffbauer et al. [3], investigated also the dependence of the direction of the laser polarization upon the angular recoil distribution of the dissociation products, which showed an absence of such dependence [3,10]. One would be tempted to conclude from this observation that the ethylene dimer is floppy and consequently that it possesses a mixed character (between $\parallel$ and $\perp$) for its transition dipole moment. However, when a small fraction of all energy is released into translation, as shown by Zare [20], it is possible to have a pure character for the transition dipole moment ($\parallel$ or $\perp$) and no influence of polarization. This is believed to be the case for CO_2-laser excitation of ethylene dimers.

5. Conclusions

The orientational hole burning for dimer predissociation can often be described by very simple expressions. The limiting cases of parallel and perpendicular transitions have been discussed.

In practice, combinations of both transitions can occur (hybrid bonds) leading to results intermediate to those displayed in fig. 1. Furthermore, the approximation $J,\ M_J \gg K,\ 1$ loses its validity for lighter systems where the 3-j symbols have to be retained and the spatial average has to be calculated numerically. Already for $(C_2H_4)_2$, one finds significant corrections [21].

* A preliminary study [7] reported a non-exponential dependence of $\bar{R}_i$ upon the laser fluence for fig 3 However, as can be concluded from a more detailed study [8], contributions of large clusters (trimers etc) are responsible for the observed peculiar fluence dependence

Acknowledgement

We acknowledge K. Janda, W.R Gentry, C Giese, J.M. Lisy and M. Hoffbauer for helpful discussions.

References

[1] T F Gough, R E Miller and G Scoles, J Chem Phys 69 (1078) 1588 85 (1981) 277
[2] M Hoffbauer, W R Gentry and C Giese, in Laser induced processes in molecules, Springer Series in Chemical Physics, Vol 6, eds K Kompa and S Smit (Springer, Berlin, 1978)
[3] M Hoffbauer, K Liu, C Giese and W R Gentry, J Chem Phys 78 (1983) 5567
[4] A Sudbo, P A Schulz, Y T Lee and Y R Chen, Proceedings of the First International School on Laser Applications to Atoms, Molecules and Nuclear Physics, Vilhuis, USSR, 1978
[5] M F Vernon, J M Lisy, D J Krajnovich, A Tramer, H S Kwok, Y R Shen and Y T Lee, Faraday Discussions Chem Soc 73 (1982) 387
[6] M P Cassasa, D S Bomse, J L Beauchamp and K C Janda, J Chem Phys 72 (1980) 6805,
M P Cassasa, F G Celii and K C Janda, J Chem Phys 76 (1982) 5295
[7] J Geraedts, S Setiadi, S. Stolte and J Reuss, Chem Phys Letters 78 (1981) 277
[8] J Geraedts, S Stolte and J Reuss, Z Physik A 304 (1982) 167
[9] J Geraedts, M Waayer, S Stolte and J Reuss, Faraday Discussions Chem Soc 73 (1982) 375
[10] D S Bomse, J B Cross and J J Valentini, J Chem Phys 78 (1983) 7175
[11] P Melinon, R Monot, J M Zellweger and H van den Bergh, Chem Phys 84 (1984) 345
[12] A R Edmonds, Angular momentum in quantum mechanics (Princeton Univ Press, Princeton, New York, 1957)
[13] J H Ling and K R Wilson, J Chem Phys 65 (1978) 881
[14] M S de Vries, V I Srdanov, C P Hanrahen and R M Martin, J Chem Phys 78 (1983) 5582
[15] R Altkorn and R N Zare, Ann Rev Phys Chem 35 (1984), to be published
[16] M Cassasa, D Bomse and K C Janda, J Chem Phys 74 (1981) 5044
[17] J Geraedts, Thesis, Katholieke Universiteit Nijmegen, The Netherlands (1983)
[18] K C Janda, Advan Chem Phys , to be published
[19] M P Cassasa, Thesis (1983) Caltech
[20] R N Zare, Mol Photochem 4 (1972) 1
[21] M P Cassasa, C M Western and K C Janda, to be published

Dit proefschrift bestaat uit vijf artikelen over de interactie van infrarood straling (9 - 11 μm) met moleculen en clusters. Het eerste artikel is het resultaat van twee werkbezoeken van in totaal vier maanden aan het Laboratorio di Spettroscopia Molecolare, in Frascati, Italië. Met een continu verstembare CO_2 TE laser werden SiH_4 moleculen geëxciteerd in een één of meer-foton proces. Door de laser frequentie in stappen van 0.06 cm^{-1} te variëren werd een absorptie-spectrum opgenomen in een lage druk opto-acoestische cel. Na vergelijking met het lineaire absorptie spectrum van SiH_4, konden de meer-foton-overgangen worden geidentificeerd. Berekeningen van C.I. and G. Pierre [1] maakten het mogelijk verscheidene twee-foton overgangen toe te kennen.

De rest van het proefschrift beschrijft het onderzoek aan kleine clusters verricht in Nijmegen. Een molecuul-bundel werd loodrecht gekruist met straling van een CO_2 laser en gedetecteerd met een bolometer. Na absorptie van een foton volgt een snel dissociatie-proces; de clusterfragmenten verdwijnen van de bundelas, zodat de totale bundelintensiteit afneemt. Zeer kleine variaties in de bundelenergie ($1{:}5 \cdot 10^6$) kunnen worden gemeten door middel van een zeer gevoelige bolometer, die zich op vrij korte afstand (400 mm) van het interaktiepunt bevindt. Door modulatie van de laserstraling was fase-gevoelige detectie van de dissociatie mogelijk. Door de laser te verstemmen konden dissociatie spectra worden verkregen. Onder de tamelijk brede (2-12 cm^{-1}) structuren die werden waargenomen gaan vele overgangen schuil, die in verband staan met de interne bewegingen in het cluster. De lijnbreedte van déze overgangen kunnen worden gerelateerd aan een ondergrens voor de levensduur van het aangeslagen cluster.

In het dimeerspectrum van C_2H_4 werden combinatiebanden van de ν_7 vibratie met een van der Waals mode waargenomen. Hot-band overgangen van dezelfde van der Waals mode werden door ons voorspeld, en zijn onlangs in Göttingen gemeten. De observatie van fijnstructuur met een lijnbreedte van 10 MHz betekende dat de levensduur van een aangeslagen C_2H_4 dimeer ten minste 16 ns is. Deze conclusie wordt ondersteund door recente berekeningen, die een levensduur van 5 μs voorspellen.

Infrarood dissociatie spectra van ammonia-dimeren tonen aan dat de twee ammonia-moleculen in het complex geen equivalene posities innemen. Een tunnel-beweging is de oorzaak van een opsplitsing van de energieniveaus in de

grond- en aangeslagen toestand van de dimeer. Deze aanname leidt tot een bevredigende verklaring van de gemeten spectra.

De structuur van de dimeren van erg symmetrische moleculen, zoals SF_6, SiF_4 en SiH_4 word hoofdzakelijk bepaald door de afstand tussen de twee moleculen. Aanname van een resonante dipool-dipool-interactie voor de geexciteerde clusters maakt een redelijke fit van de waargenomen spectra mogelijk, behalve voor SiH_4. De lijnbreedte van de pieken in de $(SF_6)_2$ en $(SiF_4)_2$ spectra kan worden gesimuleerd als men vrije rotatie van de moleculen in het complex toestaat.

We hebben ook enkele gemengde clusters onderzocht, waaronder het SiH_4-NH_3 complex.

Tenslotte zijn verzadigingseffecten voor de dissociatie van SF_6 dimeren beschreven in een theoretisch artikel.

Curriculum vitae

Op 6 januari 1959 werd ik geboren te Tilburg. Daar volgde ik een gymnasium β opleiding aan het Sint Odulphus lyceum, die in 1977 cum laude werd afgesloten. Daarna volgde de natuurkunde studie aan de Katholieke Universiteit te Nijmegen, waar in november 1980 het kandidaatsexamen en in december 1982 het doctoraalexamen in de experimentele natuurkunde (cum laude) werd behaald.

Aansluitend werd een promotie onderzoek verricht binnen de afdeling Atoom- en Molecuulfysica onder leiding van prof.dr. Jorg Reuss Tijdens dit onderzoek bezocht ik twee maal het Laboratorio di Spettroscopia Molecolare in Frascati, Italie en werkte er in totaal vier maanden. De resultaten van mijn werk in Nijmegen en Frascati worden in dit proefschrift beschreven.

STELLINGEN

1. Het werken met een intra-cavity Raman opstelling wordt vaak bemoeilijkt doordat het te onderzoeken molecuul dissocieert, bijvoorbeeld in een twee-foton proces.

2. De bewering van Richards en Barrow, later herhaald door Hocking et al., dat storingen in de hyperfijnstructuur door een interactie binnen een electronische toestand alleen zouden kunnen voorkomen in moleculen in Σ-toestanden van triplet of hogere multipliciteit, is onjuist.
D. Richards en R.F. Barrow, Nature 217 (1968) 842
W.H. Hocking, A.J. Merer en D.J. Milton, Can. J. Phys. 59 (1981) 266

3. De bekende formule voor dipool-dipool-energie, die slechts geldig is voor punt-dipolen, wordt door Pine et al. ten onrechte gebruikt voor berekening van de dipool-dipool-energie in het HF dimeer.
A.S. Pine, W.J. Lafferty en B.J. Howard, J. Chem. Phys. 81 (1984) 2939

4. De discrepantie tussen experimentele resultaten en berekeningen aan ammonia-dimeren toont aan dat ab initio berekeningen aan clusters verre van eenvoudig zijn.
D.D. Nelson Jr., G.R. Fraser en W. Klemperer, J. Chem. Phys. 83 (1985) 6201
Z. Latajka en S. Scheiner, J. Chem. Phys. 84 (1985) 341

5. Microgolfmetingen tussen 40 en 100 GHz zouden het bewijs kunnen leveren voor het voorkomen van een tunnelbeweging in ammonia-dimeren.
Dit proefschrift

6. Het door Geraedts et al. voorgestelde model voor SF_6 clusters zou getoetst kunnen worden door middel van clusterselectieve metingen, zoals verricht door Huisken et al.
J. Geraedts, M. Waayer, S. Stolte en J. Reuss, Faraday Disc. Chem. Soc. 73 (1982) 375
F. Huisken, H. Meyer, C. Lauenstein, R. Sroka en U. Buck, J. Chem. Phys. 84 (1986) 1042

7. Wanneer de overheid de arbeidskansen voor vrouwen echt wil vergroten, dient zij adequate en voldoende voorzieningen te treffen voor de opvang van baby's en kleuters.

8. Criminelen, die zich hebben schuldig gemaakt aan diefstal of vernieling, zouden de door hen veroorzaakte schade volledig moeten vergoeden.

9. De lage salarissen voor assistenten in opleiding zullen de belangstelling voor promotiebanen voor fysici doen verminderen en uiteindelijk het wetenschappelijk onderzoek aan universiteiten en hogescholen onmogelijk maken.

10. Voor een éénjarige is het erg moeilijk onderscheid te maken tussen de woorden 'pappa' (italiaans voor 'pap') en 'papa', vooral wanneer papa 's morgens de pappa brengt.

11. Het is een belediging voor de italiaanse keuken te veronderstellen dat men in Italië slechts spaghetti en macaroni nuttigt.

12. Drukkerijen drukken alles naar wens behalve de prijs.

Marcel Snels
18 juni 1986